



This is to certify that the

thesis entitled

THE CALORIMETRIC AND HARDNESS RESPONSES OF THERMOMECHANICAL TREATMENTS

IN Fe-Ni ALLOYS

presented by

Bor-Liang Chen

has been accepted towards fulfillment of the requirements for

M.S. degree in Metallurgy

Major professor

Date 5/16/86

**O**-7639

MSU is an Affirmative Action/Equal Opportunity Institution

RETURNING MATERIALS: Place in book drop to ridce in book drop to remove this checkout from your record. FINES will be charged if book is returned after the date stamped below.

10-63 17

il. Palati

# THE CALORIMETRIC AND HARDNESS RESPONSES OF THERMOMECHANICAL TREATMENTS

IN Fe-Ni ALLOYS

Ву

Bor-Liang Chen

### A THESIS

Submitted to
Michigan State University
in partial fulfillment of the requirements
for the degree of

MASTER OF SCIENCE

Department of Metallurgy, Mechanics, and Material Science
1986

#### **ABSTRACT**

# THE CALORIMETRIC AND HARDNESS RESPONSES OF THERMOMECHANICAL TREATMENTS IN Fe-Ni ALLOYS

Ву

### Bor-Liang Chen

The calorimetric and hardness responses of thermomechanical treatment in Fe-30.4%Ni alloy were systematically studied by using DSC technique, hardness measurement, X-ray diffraction, optical microstructure, scanning electron microscopy, and transmission electron microscopy. The results showed that the As and Af temperatures of reverse transformation were shifted to higher temperature side after ageing, while deformation will either increase or decrease As temperature, depending on the process performed. The enthalpy change was decreased after deforming the alloy. The hardness response of Fe-30.4%Ni alloy was remarkable. The be increased more than 80 % after ageing. hardness can The age-hardening was accomplished by the formation of fine and dense precipitates in the martensite plates.

### **ACKNOWLEDGEMENTS**

The author wishes to express his deepest appreciation and gratitude to the following people for making this phase of his graduate study possible:

To Dr. K. Mukherjee, his major advisor, for his constant encouragement and valuable guidance in this study.

To Mr. S. Sircar, for his assistance in the research and in the preparation of this thesis.

To Mr. Moti Tayal, for his friendship and help.

To his parents and wife, for their understanding, constant encouragement and endless patience.

## TABLE OF CONTENTS

	page
ACKNOWLEDGEMENTS	- ii
LIST OF TABLES	- v
LIST OF FIGURES	- vi
CHAPTER ONE: INTRODUCTION	- 1
CHAPTER TWO: LITERATURE REVIEW	- 4
2-1 The Fe-Ni Phase Diagram	- 4
2-2 The Metastable Fe-Ni Phase Diagram	- 6
2-3 Effect of Plastic Deformation on the Reverse Martensitic Transformation	- 8
2-4 Structure Changes During Reheating Fe-Ni Martensite	- 10
CHAPTER THREE: EXPERIMENTAL PROCEDURES	- 12
3-1 Materials	- 12
3-2 Thermomechanical Treatment (TMT) and Ageing	- 12
3-3 Diffrential Scanning Calorimeter (DSC) Analysis-	- 17
3-4 Retained and Transformed Austenite Determination-	- 19
3-5 Hardness Measurement	- 19
3-6 Optical and Scanning Electron Microscope Observation	- 20
3-7 Transmission Electron Microscope (TEM) Observation	- 20
CHAPTER FOUR: RESULTS	- 21
4-1 Calorimetric ResponsesDSC Measurements	- 21
4-2 Formation of Austenite	- 30

	Page
4-3 Hardness Responses	30
4-3-1 The Effect of Nickel Content and Temperature	30
4-3-2 The Effect of Deformation	37
4-4 Microstructures	40
4-4-1 Microstructures of Martensite	40
4-4-2 The Effect of Ageing on Microstructures	44
4-4-3 Formation of Austenite	49
4-4-4 Identification of Precipitates	49
CHAPTER FIVE: DISCUSSIONS	54
5-1 The Effect of Deformation on the As Temperature	54
5-2 The Effect of Ageing on The As and Af Temperature	57
5-3 The Effect of Deformation on The Enthalpy Change	58
5-4 Age-hardening Mechanism	58
CHAPTER SIX: CONCLUSIONS	60
BIBLIOGRAPHY	62

# LIST OF TABLES

Table		Page
1.	Chemical composition of Fe-30.4%Ni (wt.%)	12
2.	Hardness response data of processing in Fe-30.4%Ni	31



### LIST OF FIGURES

Figure		Page
1.	Fe-Ni binary phase diagram	• 5
2.	Metastable Fe-Ni binary phase diagram	. 7
3.	The Ms-As temperature determined by resistance measurement	9
4.	Schematic diagram of process A	14
5.	Schematic diagram of process B	15
6.	Schematic diagram of process C	16
7.	DSC thermogram of phase transformation	18
8.	DSC thermograms of reverse martensitic transformation in Fe-30.4%Ni alloy	22
9.	DSC curves of reverse martensitic transformation in deformed Fe-30.4%Ni alloy (process A)	23
10.	DSC curves of reverse martensitic transformation in deformed Fe-30.4%Ni alloy (process B&C)	24
11.	As-Af temperatures as a function of ageing time and ageing temperature (undeformed alloy)	26
12.	As-Af temperatures as a function of ageing time and ageing temperature(process A deformed alloy)	27
13.	As-Af temperatures as a function of ageing time and ageing temperature(process B deformed alloy)	28
14.	Enthalpy change of reverse martensitic transformation as a function of % deformation	29
15.	Volume fraction of austenite as a function of ageing time and ageing temperature	33
16.	Hardness responses of undeformed Fe-Ni alloys as a function of ageing time and Ni content (430°C ageing)	34

Figure	Pa	age
17.	Hardness response of undeformed Fe-30.4%Ni as a function of ageing time and ageing temperature	35
18.	Hardness response of undeformed Fe-30.4%Ni alloy as a function of ageing temperature and ageing time	36
19.	Hardness responses in Fe-30.4%Ni alloy under different processes and aged at 335°C	38
20.	Hardness responses in Fe-30.4%Ni alloy under different processes and aged at 430°C	39
21.	Optical microstructure of as-quenched Fe-30.4%Ni alloy	41
22.	TEM microstructure of as-quenched Fe-30.4%Ni alloy	41
23.	Optical microstructure of martensite obtained by process A, 70% cold rolled	42
24.	TEM microstructure of martensite obtained by process A with 70% cold rolled	42
25.	Optical microstructure of martensite obtained by process B with 70% cold rolling	43
26.	TEM microstructure of martensite obtained by process B with 70% cold rolling	43
27.	TEM microstructure of martensite obtained by process C with 70% cold rolling	45
28.	Precipitates formed in the martensite after ageing the undeformed sample at 335°C, 500 h	45
29.	Typical precipitates formed after ageing at 335°C for 1000 hours	46
30.	Precipitates were coarsened when aged at 430°C for 1000 hours	46
31.	Cellular precipitation in an Fe-30.4%Ni aged at 430°C for 1000 hours (TEM)	47
32.	Cellular precipitation in an Fe-30.4%Ni aged at 430°C for 1000 hours (SEM)	47

;

Figure	F	age
33.	Microstructure of aged Fe-30.4%Ni martensite, processA with 70% cold rolling, aged at 335°C, 1000 h	48
34.	SEM microstructure of aged martensite, process B with 70 % cold rolling, aged at 335°C, 1000 h	48
35.	SEM microstructure of aged martensite, process C with 70 % cold rolling, aged at 335°C, 1000 h	50
36.	Austenite formed by diffusional process, process B aged at 430°C for 1000 hours	50
37.	Austenite formed by diffusional process, after ageing at 430°C for 1000 hours in process C	51
38.	Austenite formed by diffusionless and diffusional processes, after ageing at 430°C for 1000 hours in process A	51
39.	TEM microstructure of Fe-30.4%Ni alloy shows austenite formed by diffusionless process after aged at 430°C for 1000 hours in process A	52
40.	Precipitates formed in the grain boundary	52
41.	The free energy of Fe-Ni martensite and austenite as a function of temperature (Schematic)	55

#### CHAPTER ONE

#### INTRODUCTION

In the Fe-Ni phase diagram proposed by many researchers [1-5] there exists a vast two-phase  $(\alpha + \gamma)$  region extending from 910 C to below room temperature. It is well known [1] that the diffusion rate of Ni atoms in Fe is so low that an Fe-Ni alloy, when cooled from the austenite field and held at a temperature within the two phase region, usually will not decompose to equilibrium  $\alpha$  and  $\gamma$  phases but will transform to martensite on further cooling. Furthermore, when the nickel content is greater than 28 at. %, the Fe-Ni austenitic alloy will not transform to martensite until cooled down to below 7°C [6]. Because of these characteristics, Fe-Ni alloys have been widely used in the study of martensitic transformations in the past decades. Most of these studies were concentrated with the morphology, crystallography and substructures of Fe-Ni martensites. Comparatively few reports were on the strengthening calorimetric response and effects deformation and thermal treatment in this alloy system.

The Fe-Ni martensites are relatively soft and ductile

in the as-quenched condition, due to the low solid solution hardening effect of the substitutional element Ni [7]. Therefore, they can be easily deformed at room temperature. Some researchers have studied the effects of deformation and thermal treatment on the martensitic transformations and microstructures of these alloys [8-10]. Pope [8] reported the austenite start temperature of an Fe-30.3% Ni-0.005% C alloy increases monotonically with plastic deformation introduced by cold rolling, and attributed this effect to the increase in yield stress of martensite. Furubayashi et al [9] investigated the microstructures of Fe-Ni martensites after being cold rolled and annealled at various temperatures in the two phase region, and concluded that microduplex structures (composed of and grains of submicron size) can be formed by this treatment for Fe-Ni alloys with nickel content of 13 % - 22 %. This observation seems to be in agreement with that of Miller [10].

Recently, the technique of differential scanning calorimeter (DSC) has been applied to investigate the phase transformation of Fe-Ni alloy [11]. By using DSC Chang et al showed that the As and Af temperatures and the enthalpy change of reverse martensitic transformation in an Fe-24% Ni alloy were affected by heat treatment. The As and Af temperatures are all shifted to higher temperature side after ageing at 450°C and 490°C. Their study prove that DSC is an effective tool for phase transformation study.

The age-hardening phenomenon in binary Fe-Ni martensitic alloys was reported by Leslie and Miller [12]. They observed that Fe-Ni martensites, containing about 28 to 34 wt. % Ni, can be remarkably hardened by thermomechanical treatment. They also found that the hardening is accomplished by formation of a high density of fine precipitates in the martensite plates. But they did not identify the precipitates.

The purpose of the present work is to confirm the age-hardening behavior of Fe-Ni alloys with nickel content of 27.7 to 30.4 wt. %, and to study the calorimetric and hardness responses of various thermomechanical treatments in these alloys, and thereby to infer their possible hardening mechanism. This study was accomplished by DSC analysis, X-ray diffraction test, hardness measurement, optical microscopy, scanning electron microscopy (SEM) and transmission electron microscopy (TEM).

### CHAPTER TWO

### LITERATURE REVIEW

The basic properties of Fe-Ni alloy with nickel content of 27.7 to 30.4 wt. % are directly related to the characteristics of the iron-rich end of the iron-nickel phase diagram. Therefore, it is worthwhile to survey the low temperature (below 1000°C) Fe-Ni phase diagram in order to understand the effect of deformation and thermal treatment on the microstructure and properties of Fe-Ni alloys. There are two diagrams to be considered. One is the equilibrium diagram and the other is the metastable equilibrium diagram.

### 2-1 The Fe-Ni Phase Diagram

The generally accepted Fe-Ni phase diagram is that due to Owen and Liu [2] as shown in Figure 1. Several modifications to this diagram have been proposed by some researchers [3-5], which were also shown in Figure 1.

One feature of low temperature Fe-Ni phase diagram is its comparative simplicity; there being present only two pure phases, namely, the  $\alpha$  and  $\gamma$  phases. Above 910°C, there is a region of complete solid solution,  $\gamma$  (fcc) phase.

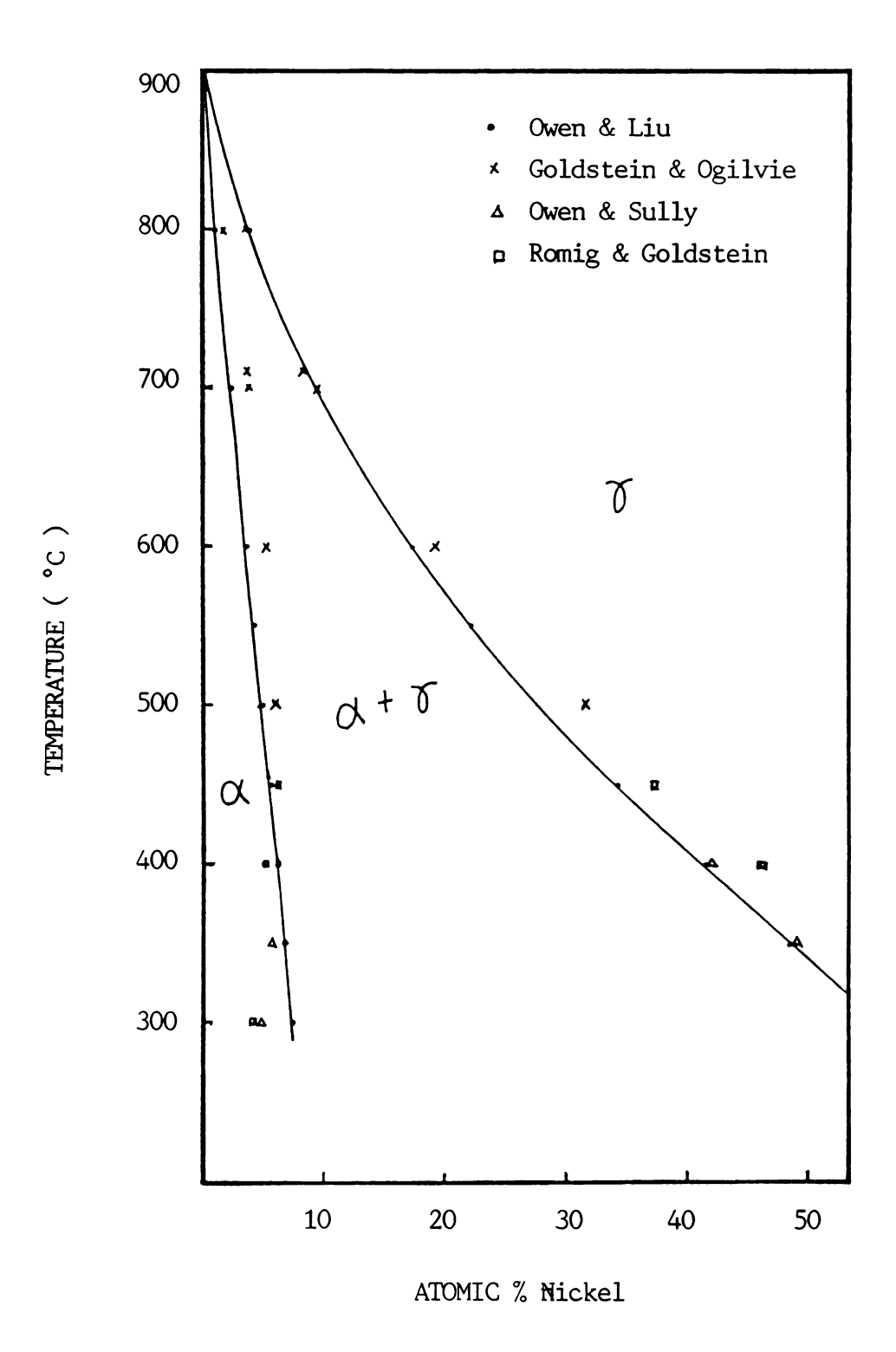


Figure 1. Fe-Ni binary phase diagram

Below 910°C, the  $\alpha$  (bcc) phase is stable in pure iron. The effect of increasing amounts of nickel is to stabilize the phase. It is well known that upon cooling an alloy from the austenite state and held at a temperature within the  $\alpha+\gamma$  state for a very long time, the austenite usually will not decompose into the equilibrium austenite and ferrite compositions. Instead, the austenite will transfer to a supersaturated martensite with a bcc crystal structure on further cooling. The equilibrium  $\alpha$  and  $\gamma$  phases can be approached if the martensite is heated in the two phase region and held for a long time.

Some researchers [5,13,14] have reported ordered phases including FeNi and FeNi in the Fe-Ni alloy system. Keumann and Karsten [5] observed that the fcc Fe-Ni solid solution decomposed eutectoidally at 345°C and 52 at. % Ni to a mixture of FeNi<sub>3</sub> and  $\alpha$ -Fe. Kaufman and Nesor [13] also predicted the  $\gamma \longrightarrow \alpha$ +FeNi<sub>3</sub> eutectoid reaction to occur at 345°C. Knudsen et al [14] observed an ordered FeNi phase in the iron-nickel alloy system.

### 2-2 The Metastable Fe-Ni phase diagram

The metastable Fe-Ni phase diagram as shown in Figure 2. was proposed by Jones and Pumphrey [15]. From this figure, it can be seen that if an Fe-Ni alloy is cooled from the  $\gamma$  state to low enough temperature it will transform to martensite. If, then, the martensite is reheated, one of two things may happen. If it is reheated

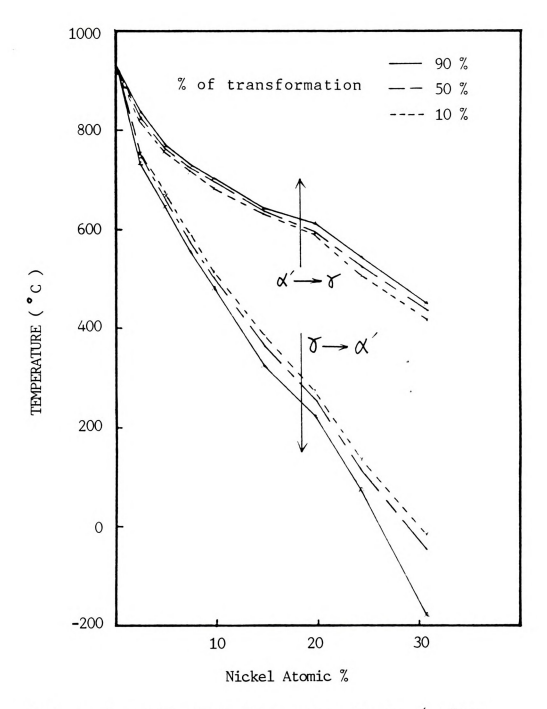


Figure 2. Metastable Fe-Ni binary phase diagram ( after Jones & Pumphrey [15] ).

to a temperature below the As temperature the martensite will decompose into the equilibrium austenite and ferrite compositions, i.e. the martensite reverts to the equilibrium phases given in Figure 1. If, on the other hand, the martensite is heated above the As temperature, it transforms back to an austenite of the same composition by a shear reaction.

The martensite start temperature Ms and austenite start temperature As have been determined by resistancetemperature measurements at a cooling or heating rate of 5°C per min. by Kaufman and Cohen [6] and is shown in Figure 3. This figure indicated that in alloys with nickel content 28 at. % the austenite phase is retained at room They claimed that temperature. the transition temperatures are rather insensitive to the heating or cooling rate. While other researchers [ 11 ] have shown that the As temperature was affected by heating rate. The As temperature decreased as the heating rate increased.

# 2-3 <u>Effect of Plastic Deformation on The Reverse</u> Martensitic Transformation

It has been reported [16] that when Fe-Ni austenite is plastically deformed at room temperature, residual stresses and lattice defects will be introduced. The residual stresses will lower the As temperature. The effect of residual stresses on As temperature increases with

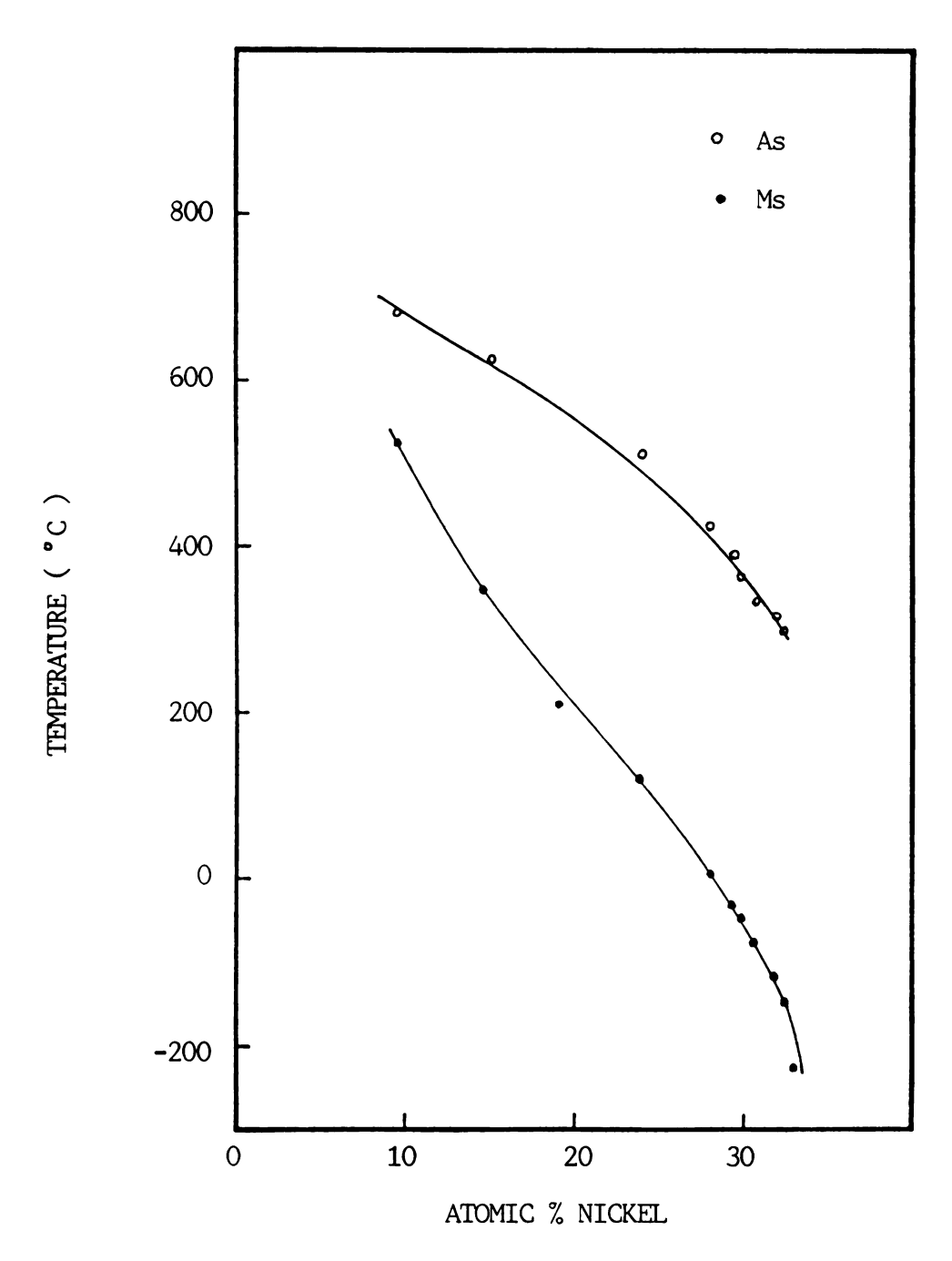


Figure 3. The Ms-As temperature determined by resistance measurement ( after Kaufman and Cohen [6] ).

increasing degree of deformation. On the other hand, lattice defects raise the austenite finish temperature. Thus the temperature range of transformation is widened by deforming the austenite before quenching to form martensite.

In a study of the effect of plastic deformation on the martensite-to-austenite transition in an Fe-30.3%Ni-0.005%C alloy, Pope [8] reported that when plastic deformation was performed on the martensite at room temperature, the austenite start temperature As increased monotonically with deformation. He attributed this effect to the increase in yield strength of martensite due to plastic deformation.

### 2-4 Structure Changes During Reheating Fe-Ni Martensite

Many investigators have observed the structure changes during reverse martensitic transformation. Cohen and Kaufman [17] reported that the reversal of Fe-Ni martensite took place both at the edge of martensite plate and in a piecewise fashion within them. Wayman and Jana studied the reverse transformation of an Fe-33.95%Ni alloy. They observed that the reversal began at the martensite-austenite interface and the midrib disappeared relatively early during reversal. They also observed that some of the martensite plates exhibits a partial loss of transformation twins between 200°C and 280°C on slower heating. Therefore, they concluded that a diffusion-controlled reversal process

occurred simultaneously with a diffusionless process. Cohen reported that the distortions and [19] imperfections produced in Fe-Ni austenites by the reverse martensitic transformation resulted in appreciable strengthening. They observed that the reversal started at the periphery of the martensitic plate, but subsequently the plates break up in a piecewise fashion. Krauss and [20] observed that small island-shape reversed austenites have different orientation from that of the original austenite. They also observed high density of tangled dislocation with interspersed loops in the reversed austenites. Kessler and Pitsch [21] studied the reverse transformation of an Fe-32.5%Ni alloy, and reported that the austenite phase initiated in small regions along the austenite/martensite interfaces.

### CHAPTER THREE

:

### EXPERIMENTAL PROCEDURES

### 3-1 Materials

Three Fe-Ni alloys were used for the present study.

The Ni contents of the alloys were 30.4% Ni (alloy A),

29.2% Ni (alloy B) and 27.7% Ni(alloy C) respectively. The

'as-received' materials were hot-rolled 1/2 in. by 1/2 in.

square bars. All materials were normalized at 900°C for 24

hours before performing thermomechanical treatment. The

chemical analysis of Fe-30.4% Ni alloy is listed in Table 1.

Table 1. Chemical Composition of Fe-30.4%Ni (wt.%)

Ni	С	Ti	Al	Fe
 30.4	0.015	0.037	0.038	balance

### 3-2 Thermomechanical Treatment(TMT) and Ageing

Three kinds of TMT process were performed in this study. Process A is in the category of class I TMT proposed by Radcliffe and Kula [ 22 ], and process B is in the category of class III TMT. Process C is the process in

which materials are requenched in liquid nitrogen after being performed by process B.

In process A, the alloys were first reheated to 900°C, held for 2 hours and cooled to room temperature, and then deformed. Deformation(cold-rolling) was performed in multiple passes by rolling at room temperature with a reduction ratio in thickness of 10%, 40%, and 70%. After deformation, the alloys were quenched in liquid nitrogen to -196°C for 20 minutes. The materials were subsequently aged at 335°C, 400°C, and 430°C respectively in salt bath for various periods of time(25 hrs., 50 hrs., 100 hrs., 500 hrs., and 1000 hrs.), and then quench in water.

In process B, the alloys were first reheated to 900°C, held for 2 hours, and cooled in brine to room temperature, and then quenched in liquid nitrogen to -196°C for 20 minutes. After quenching, the materials were subsequently deformed at room temperature in the same way as in process A but with a reduction ratio in thickness of 0%, 10%, 40%, and 70%. Finally, the alloys were aged in salt bath at 335°C, 400°C, and 430°C respectively for 25 hrs., 50 hrs., 100 hrs., 500 hrs., and 1000 hrs., and then quenched in water.

In process C, the materials with a reduction ratio in thickness of 70% obtained by process B were requenched in liquid nitrogen to -196°C before performing ageing treatment.

Schematic diagrams of processes A, B, and C are shown in Figure 4,5, and 6 respectively.

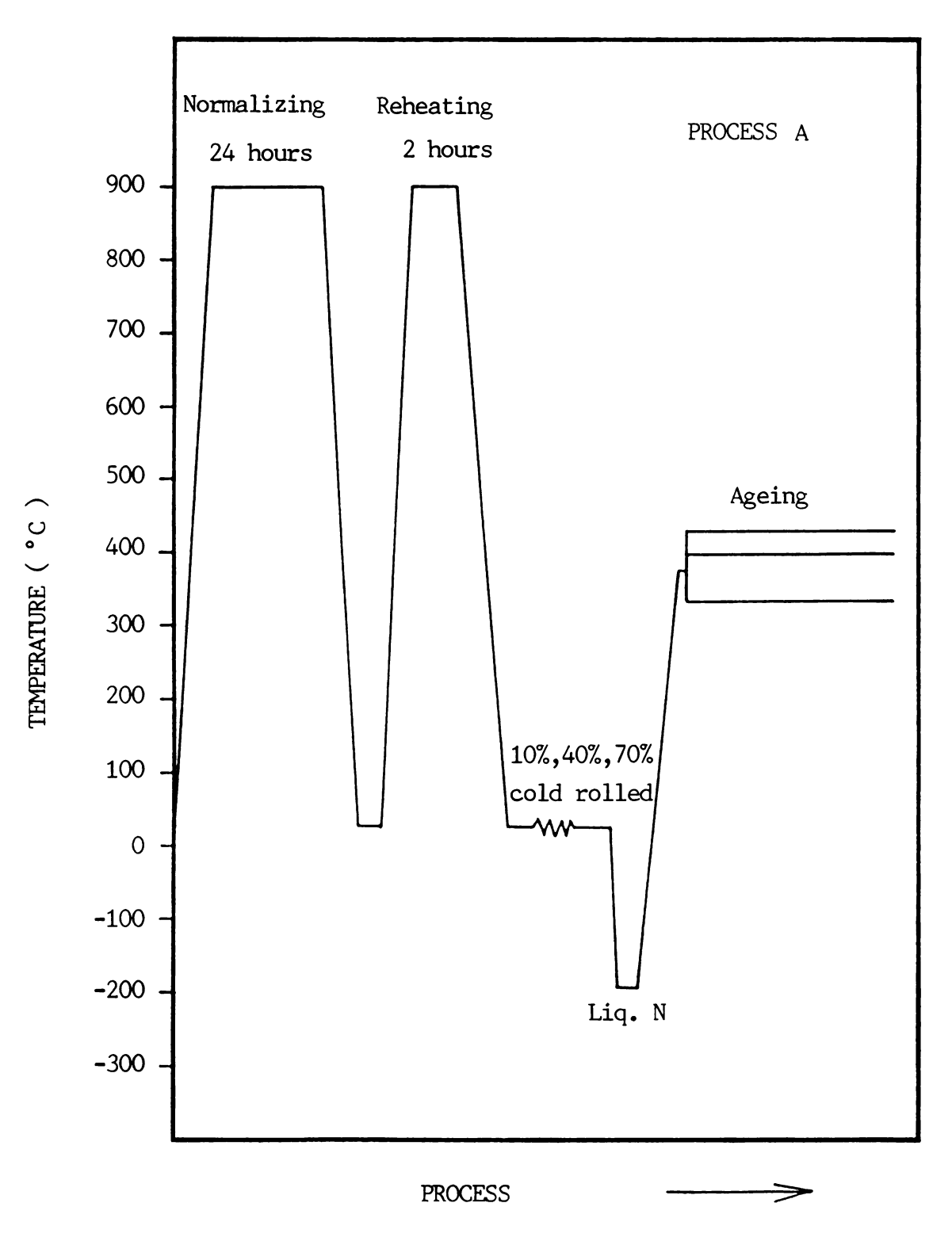


Figure 4. Schematic diagram of process A

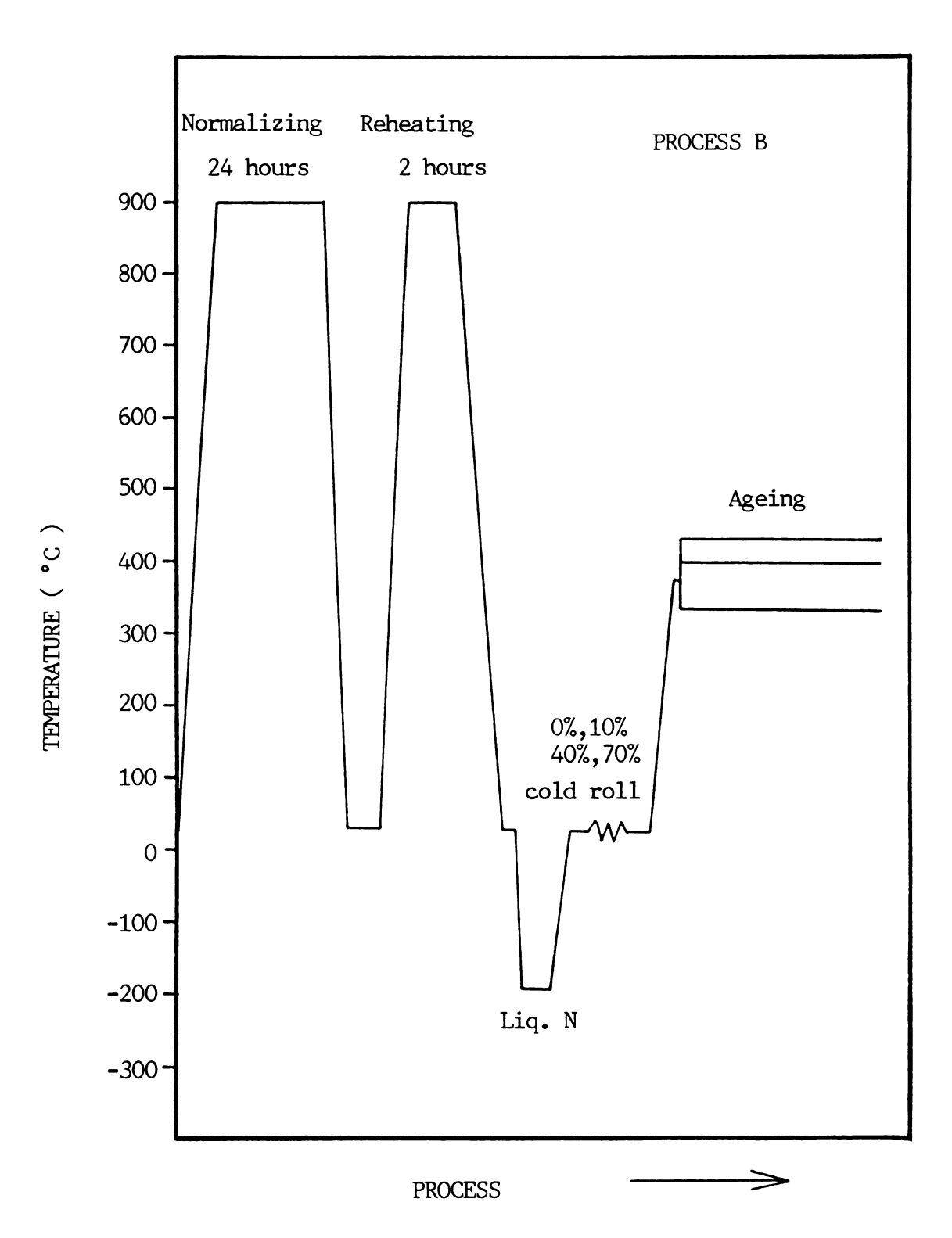


Figure 5. Schematic diagram of process B

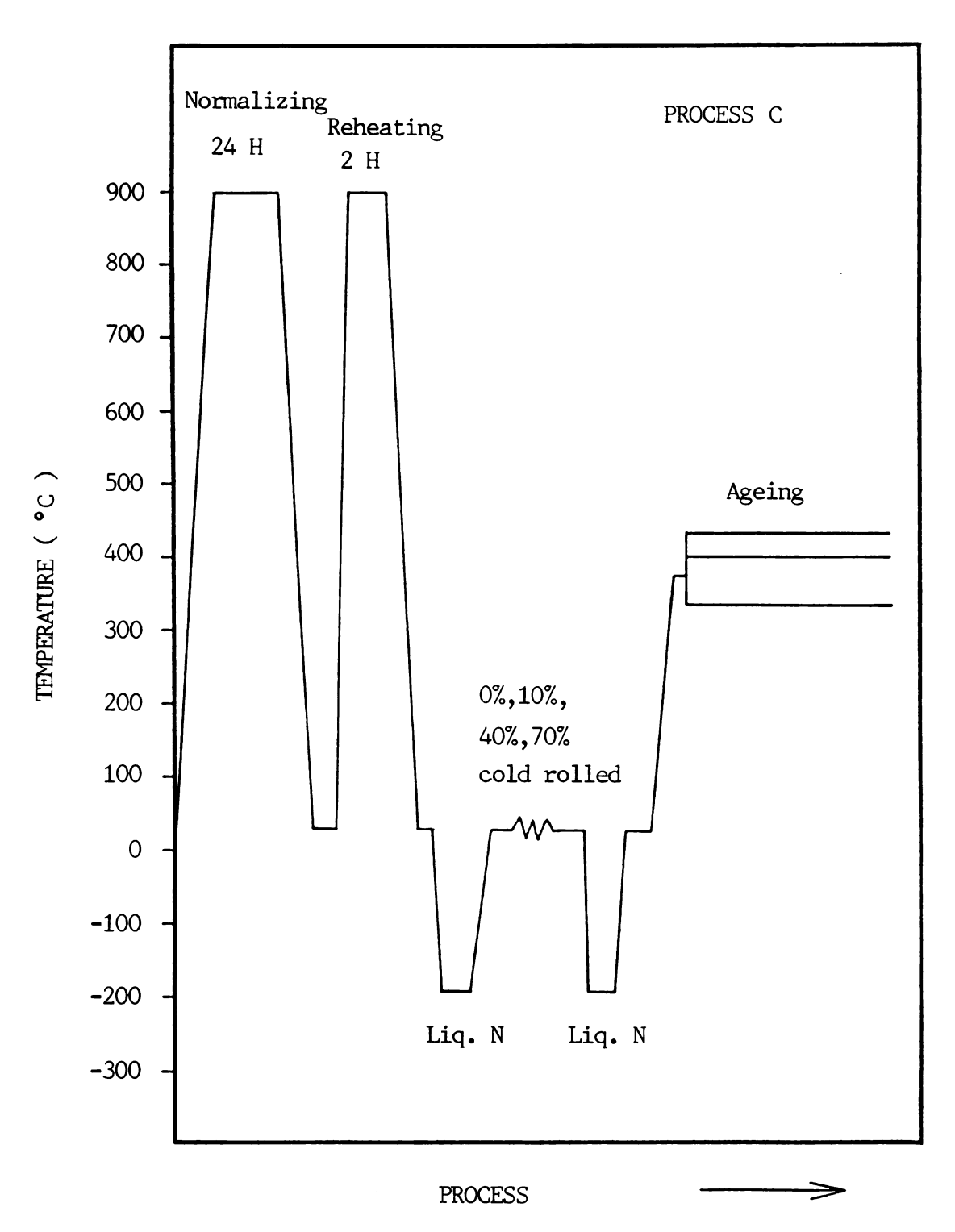


Figure 6. Schematic diagram of process C



### 3-3 <u>Diffrential Scanning Calorimeter (DSC) Analysis</u>

The phase transformation temperatures (As and Af) of varies specimens were monitor by using a DuPont 990 thermal analyzer equipped with 910 differential a scanning calorimeter (DSC) system. The calorimeter is programmed to change the average temperature of the sample pan and the reference pan(Pt.) at a constant rate, such as 10°C/min.. Differential power is supplied to keep the temperature of the sample pan equal to that of the reference pan. As average temperature changes the power supplied to the sample with respect to the reference is constant, except when the sample undergoes a phase transformation that involves latent heat. When this occurs, the power supplied to the sample and the reference is different and result in a maximum peak on the recorder trace during the phase minimum transformation. Schematic recorder traces are shown in The vertical axis corresponds to the differential power \$\Delta H/\Delta t\$, where H is enthalpy and t is time or temperature. The horizontal axis corresponds to temperature The 4H/At scale increases in the direction from the or time. to the bottom of the plot. Austenite-Martensite transformation are endothermic on heating (from martensite to austenite) and exothermic on cooling (from austenite to martensite). Thus, austenite-martensite transformations give rise to minima on heating and maxima on cooling. The tangential extrapolation method was used to define endothermic transformation temperatures As (austenite start)

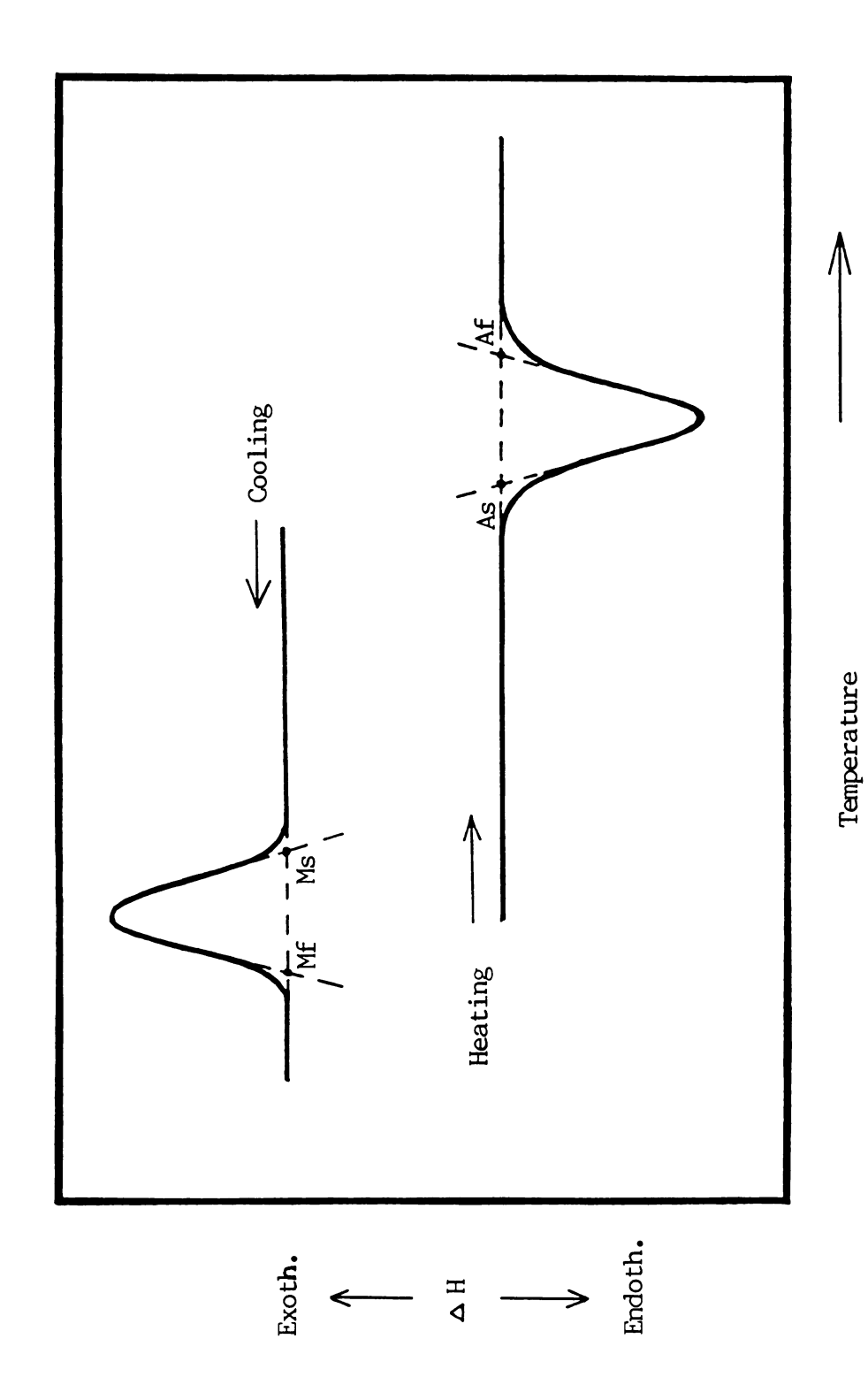


Figure 7. DSC thermogram of phase transformation.

and Af (austenite finish), as illustrated in Fig. 7. The enthalpy H of a transformation is directly proportional to the peak area which were closed by connecting the baselines as shown in Fig.7.

The DSC was operated with the sample in a chamber purged with argon gas. All scans were performed with the temperature changing at a constant rate of 20°C/min.. The calibrations of heat and temperature were performed by using the melting of indium.

### 3-4 Retained and Transformed Austenite Determination

The amount of retained austenite and the volume fraction of gamma phase precipitated during ageing of undeformed sample were determined by a method using X-ray diffractometer [ 23 ]. Because of the existance of prefered orientation, deformed samples were not tested.

### 3-5 <u>Hardness Measurement</u>

Hardness testing were carried out for all the specimens by using a Rockwell hardness tester. The specimens were prepared by being carefully polished the two opposite traverse sections, which were perpendicular to the rolling direction, to remove the possible oxidized layers. Three hardness values were measured on each specimen. The hardness values reported here are the average of three readings. Some selected specimens were also chosen to do the microhardness testing. Alloy A had the greatest hardness response and was selected for more detail study.

### 3-6 Optical and Scanning Electron Microscope Observation

Optical metallography and scanning electron microscopic examination were performed according to standard laboratory practice. They were carried out for alloy A only. The specimens were mechanically polished and etched with 5% Nital, and then examined with a LECO optical microscope and Hitachi S-415A SEM, operated at 25 KV.

## 3-7 Transmission Electron Microscope (TEM) Observation

Transmission electron microscope examinations were also carried out for alloy A only, and were performed with a Hitachi U-800 electron microscope operating at 200 KV. Slices of 0.1 mm thick were cut by using an Isomet Low Speed Diamond Saw, then mechanical thinning followed by double-jet polishing with a Tenupol-2 jet polishing machine. The electrolyte used was 10% percloric acid and 90% acetic acid solution. The voltage of electropolishing was kept at 40V. The temperature of electropolishing was kept at room temperature.

### CHAPTER FOUR

### RESULTS

### 4-1 <u>Calorimetric Responses--DSC measurements</u>

Figure 8. shows the DSC thermograms of reverse martensitic transformation for undeformed Fe-30.4% Ni alloy with or without ageing treatment. The As and temperatures of as-quenched sample are 395°C and 448°C respectively. When aged at 335°C (below the As temperature of the as-quenched sample), the endothermic reaction peak and As temperature of the reverse martensitic transformation were all shifted to higher temperature side as the ageing time increased. However, the Af temperature almost did not increase until after ageing for 100 hours at 335°C. On other hand, the As and Af temperatures increased remarkably after ageing for 25 hours at 430°C (above the As temperature of as-quenched sample).

The effect of deformation on the DSC curve was shown in Figure 9 and 10. When the alloy was deformed 10 % in thickness before quenching, the As temperature was decreased. Increase the deformation rate to 40%, As temperature was decreased further. But, further increase the deformation rate to 70%, the As temperature was raised (though still lower than that of the as-quenched sample). On

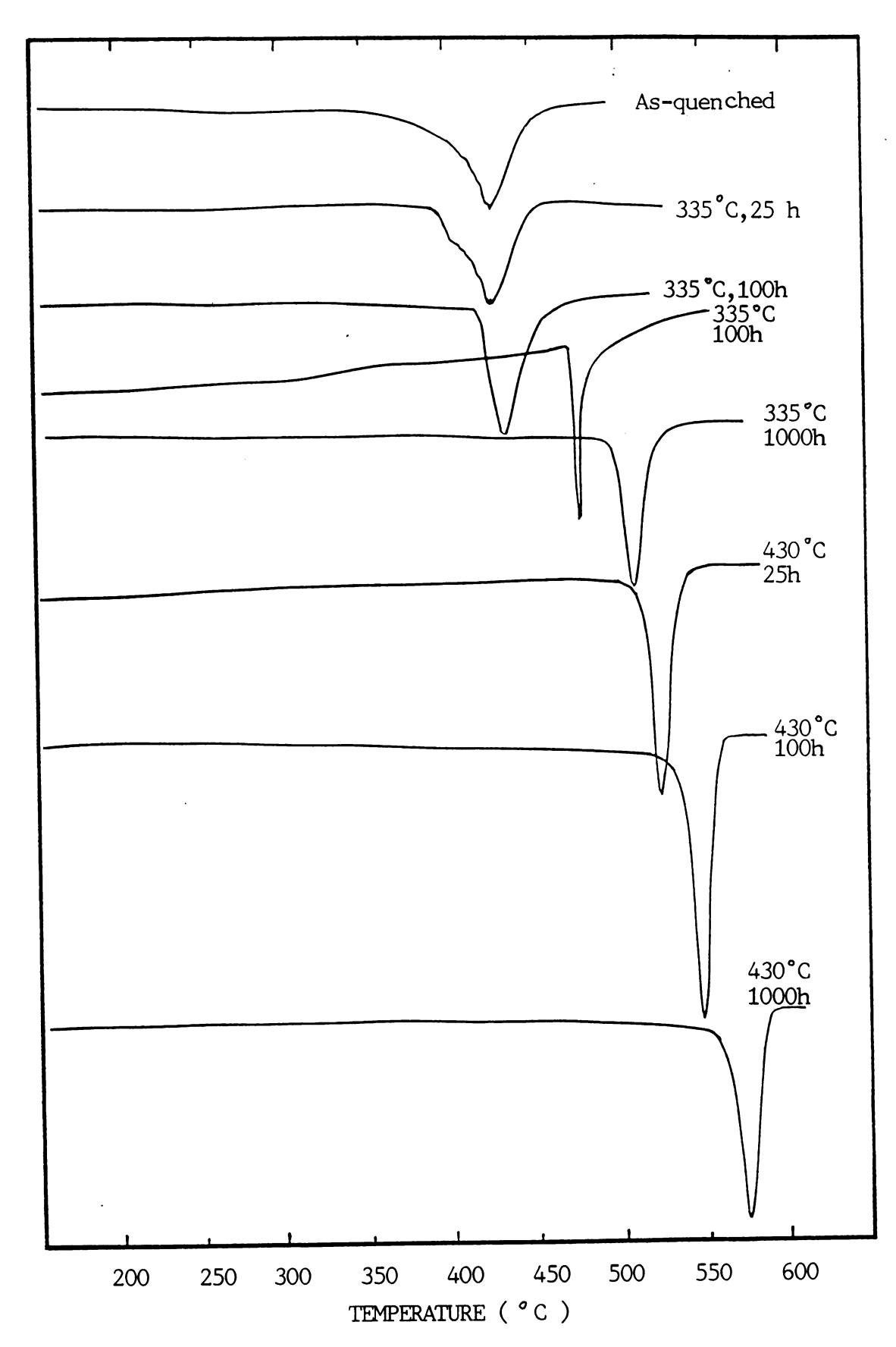


Figure 8. DSC thermograms of reverse martensitic transformation in Fe-30.4% Ni alloy.

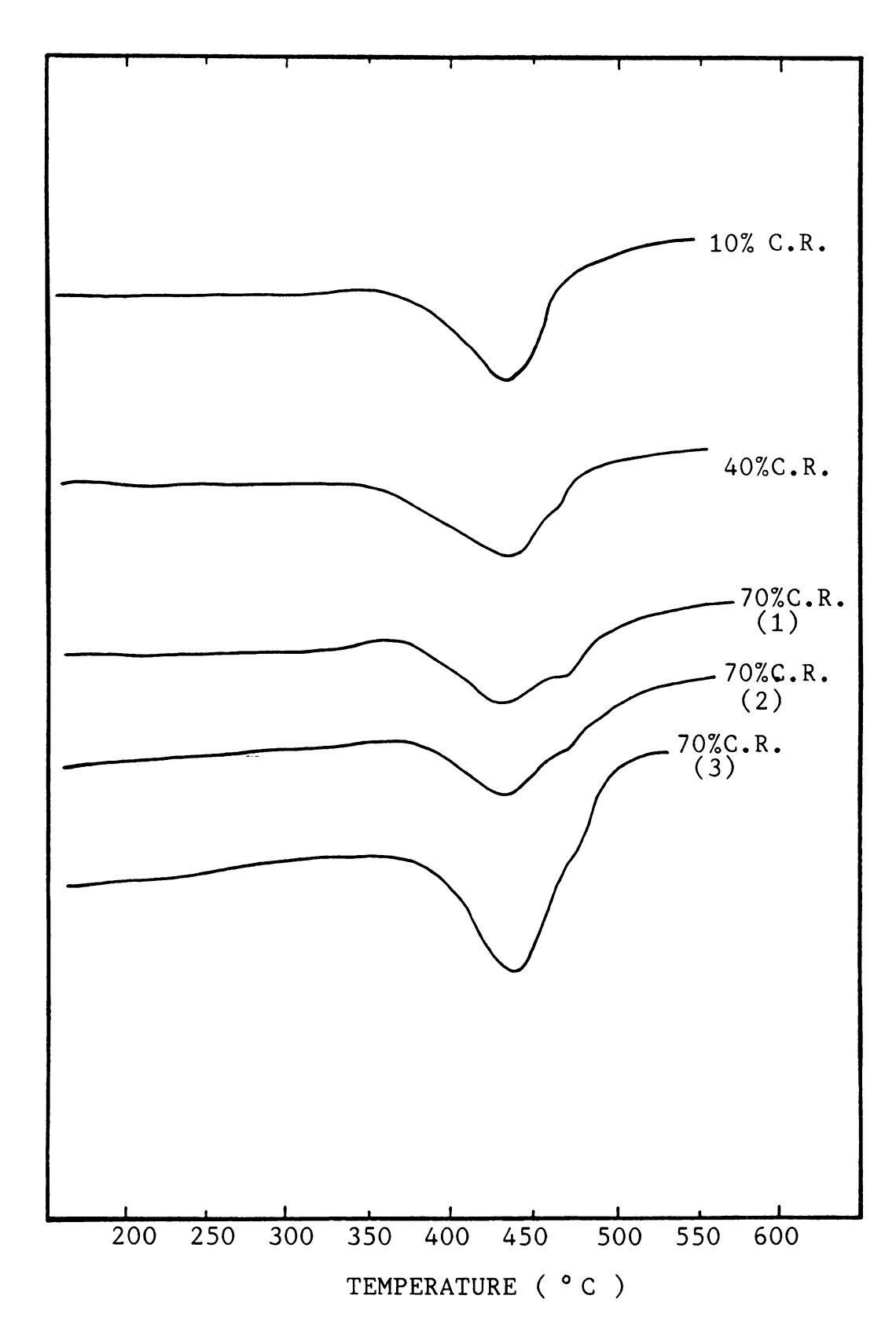


Figure 9. DSC curves of reverse martensitic transformation in deformed Fe-30.4%Ni alloy (process A).

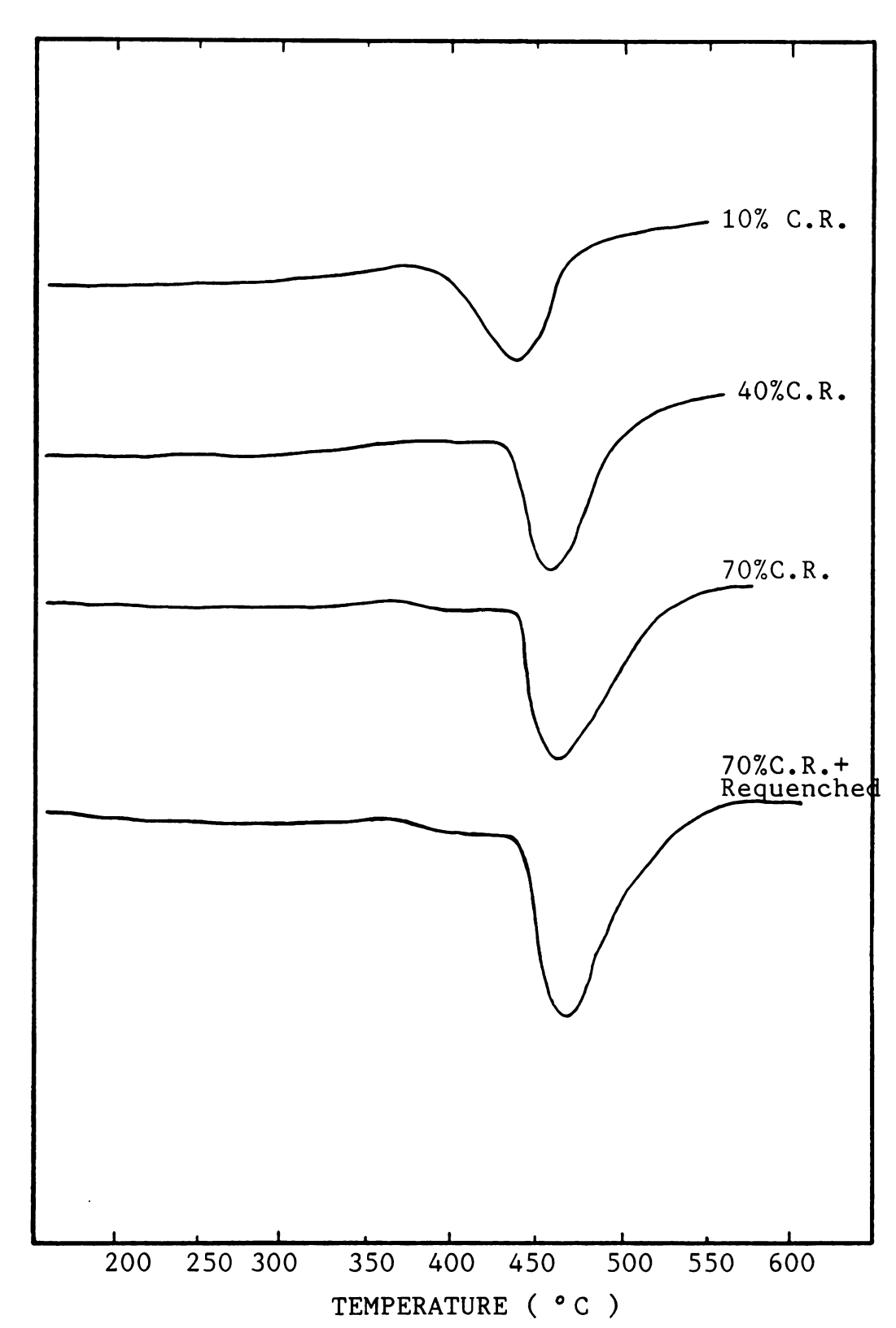


Figure 10. DSC Curves of reverse martensitic transformation in deformed Fe-30.4%Ni alloy (process B&C).

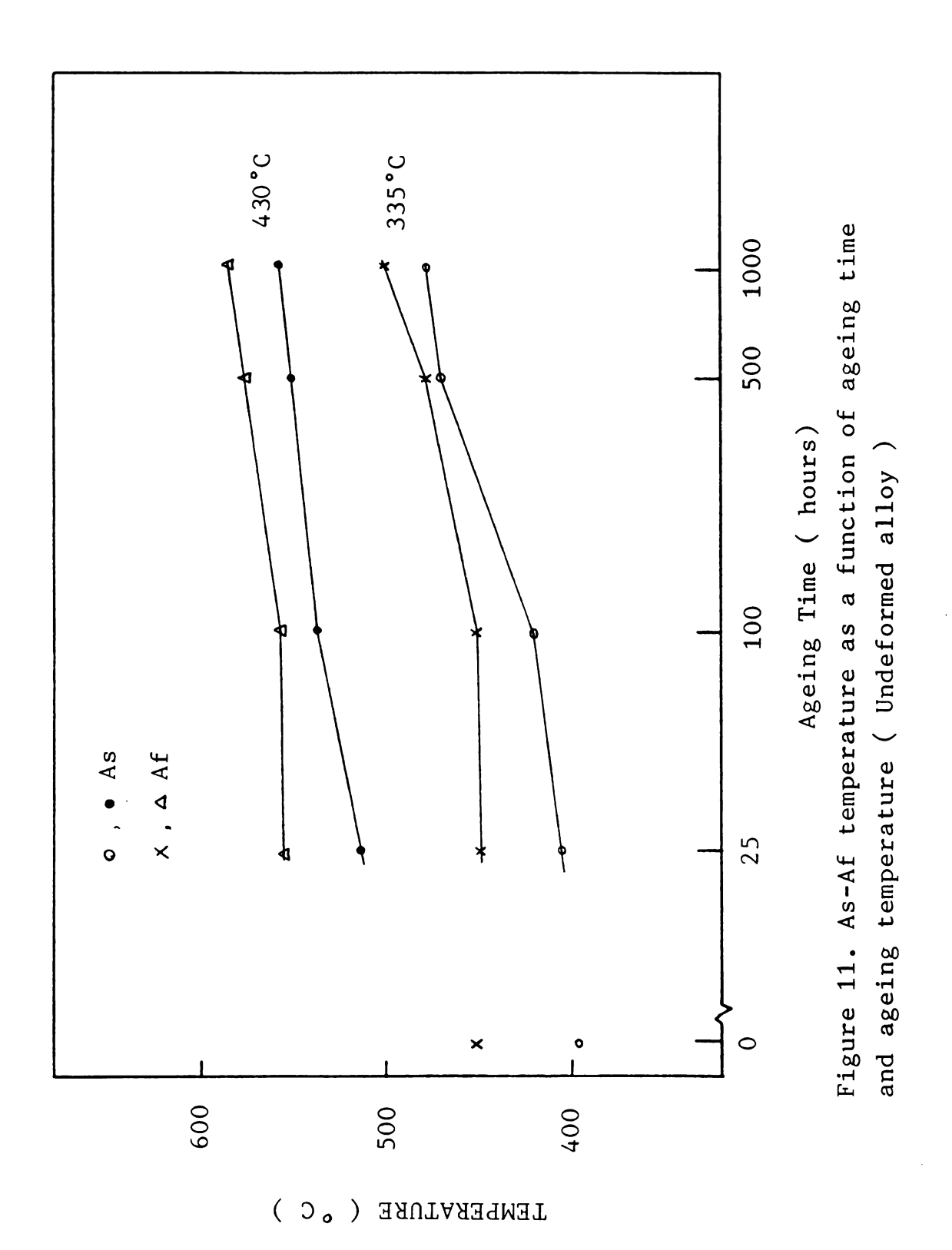


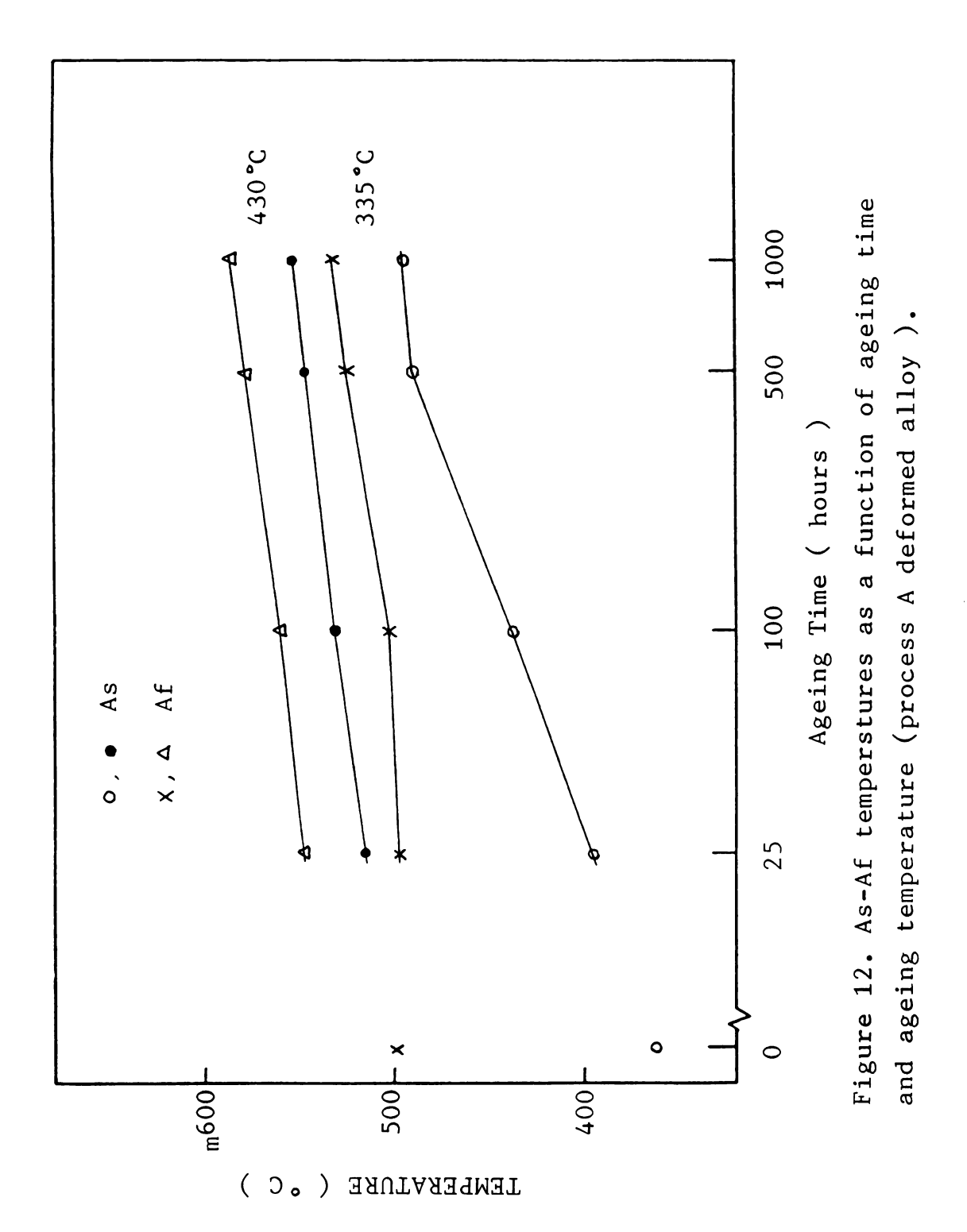
the other hand, the Af temperatures increased with the deformation rate. It can be seen from Figure 9. that a second peak occurred gradually as a result of increasing the deformation rate. When deformation was performed on the martensitic Fe-Ni alloy, the As and Af temperature were both increased as the deformation rate increased. This result is in agreement with that of Pope [8]. Although there is no second peak occurred, the temperature range between the peak temperature and Af temperature was widened by deforming the martensite.

Figure 11 to 13 show the change of As and Af temperatures with respect to ageing time and ageing temperature. It is clear that when ageing at 430°C for only 25 hours, the As and Af temperatures raised remarkably for all cases. The shape of the endothermic peaks is rather symmetry when aged at 430°C. While, when aged at 335°C the endothermic peaks generally did not become symmetry until after aged for 1000 hours, as shown in Figure 8.

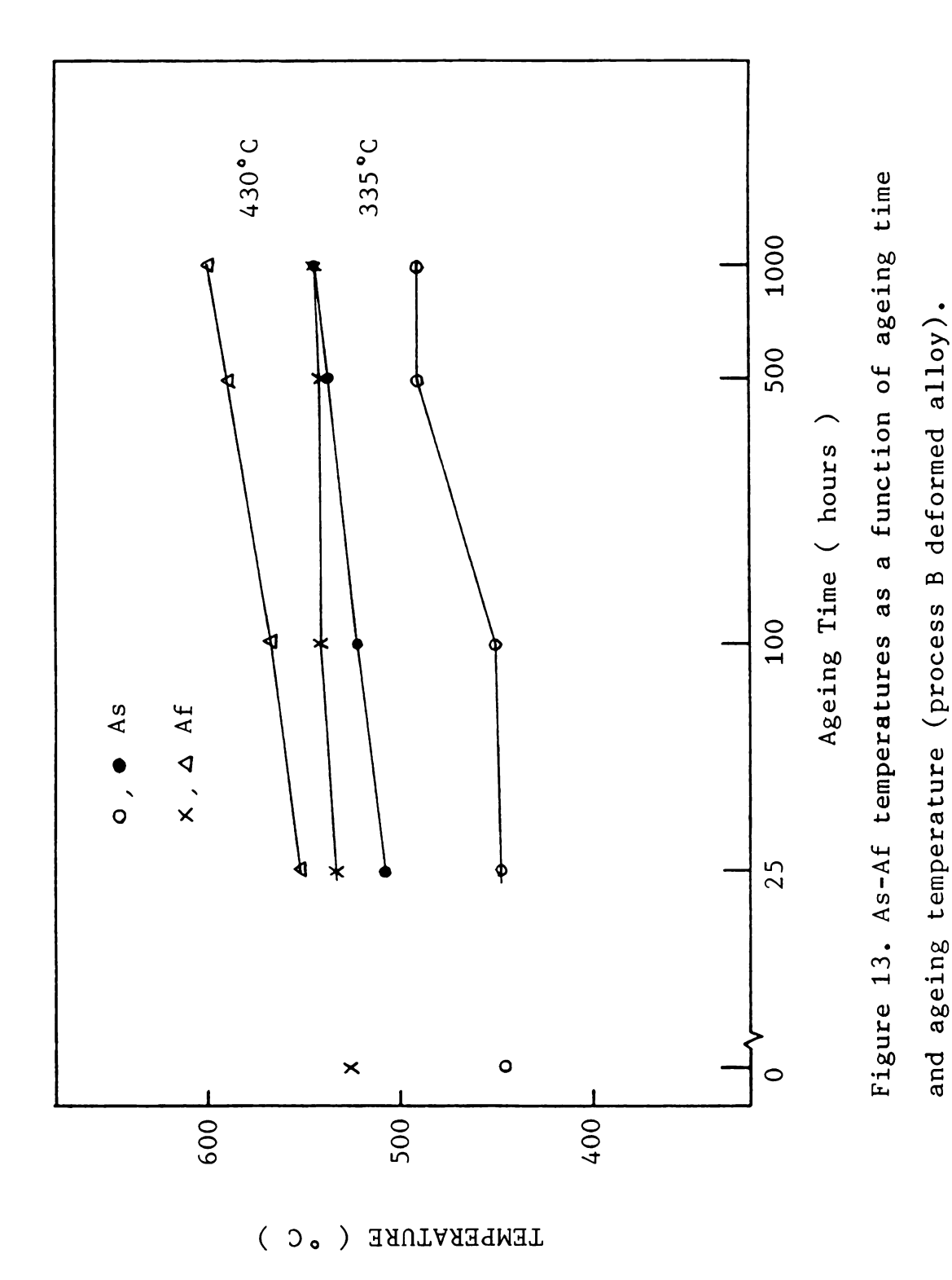
Some of the DSC curves show a relatively small exothermic peak between 300°C and 400°C (below the As temperature). This indicates that certain reaction occurred at this temperature range.

The enthalpy change of phase transformation was calculated by measuring the peak area. Figure 14. shows the effect of deformation on the enthalpy change of reverse transformation. It shows that the enthalpy change decreased as the deformation rate increased.









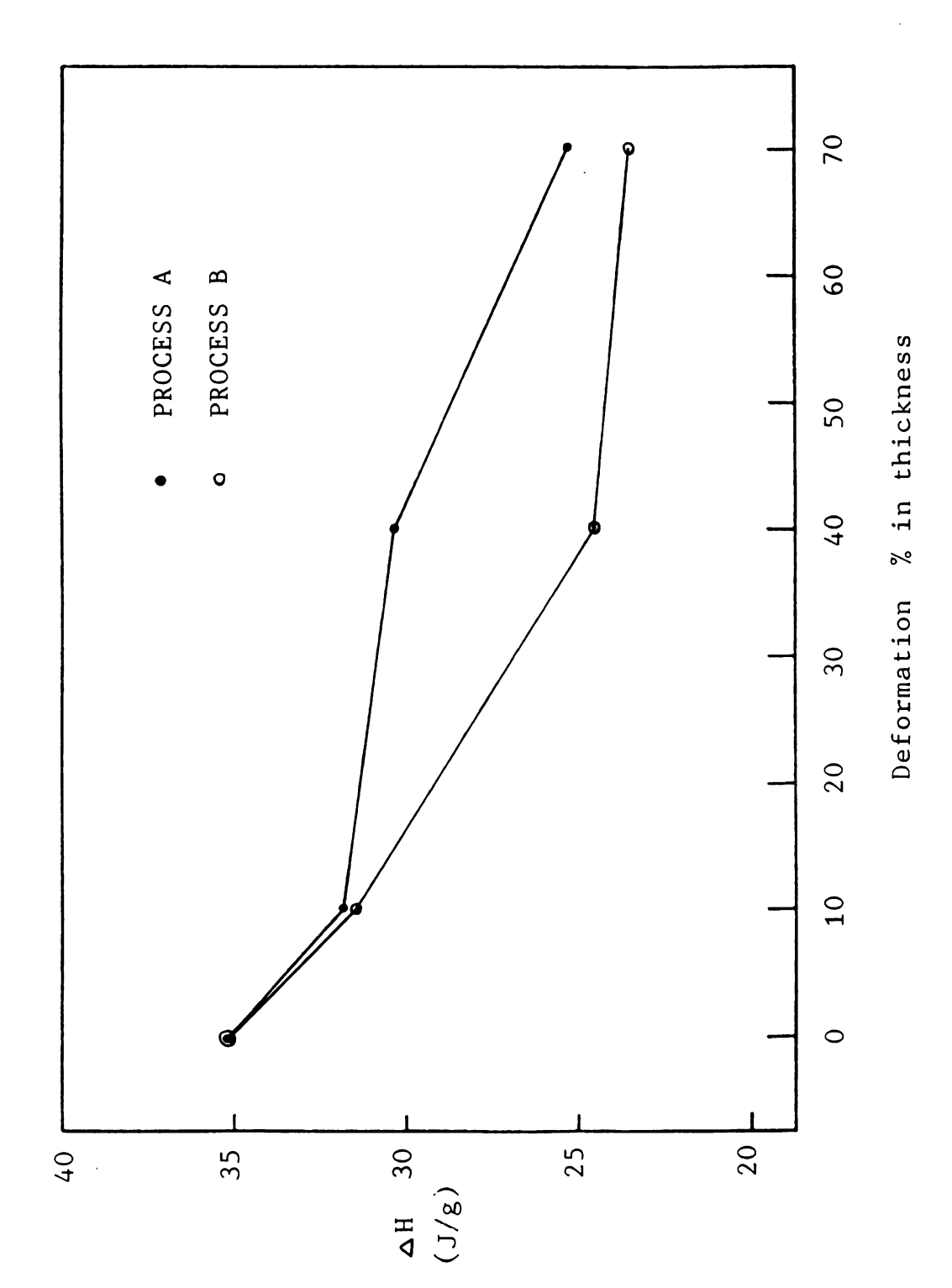


Figure 14. Enthalpy change of reverse martensitic transformation as a function of % deformation.

# 4-2 Formation of Austenite

The retained austenite contents in the as-quenched Fe-27.7%Ni, Fe-29.2%Ni and Fe-30.4%Ni alloys are 0%, 6.7% and 14.2% respectively. After ageing at 335°C and 430°C, austenite will be formed gradually as a function of ageing time as shown in Figure 15. When aged at 335°C (below As temperature), the formation rate of austenite is much slower than that of ageing at 430°C (above As temperature).

## 4-3 <u>Hardness Responses</u>

The hardness data measured in this study for Fe-30.4% Ni are listed in Table 2.

#### 4-3-1 The Effect of Nickel Content and Temperature

Fig. 16. shows the hardness changes during ageing of the undeformed Fe-30.4%Ni, Fe-29.2%Ni, and Fe-27.7%Ni martensites at 430°C. These alloys were aged in the a+r fields and all exhibited a single ageing hardness peak. This figure shows the effect of nickel content on the ageing behavior of the Fe-Ni alloys. The peak hardness the nickel content is increased from 27.7 to rises as 30.4%Ni. The time required to reach peak hardness decreases profoundly as the nickel content is increased from 27.7 to 29.2%Ni, and then slightly increases as the is increased to 30.4%Ni. Overageing content occurred after ageing for 50 hours and 100 hours at 430 °C for Fe-29.2%Ni and Fe-30.4% Ni respectively.

Fig. 17 and 18. both show the hardness responses of the undeformed Fe-30.4%Ni alloy with respect to the ageing

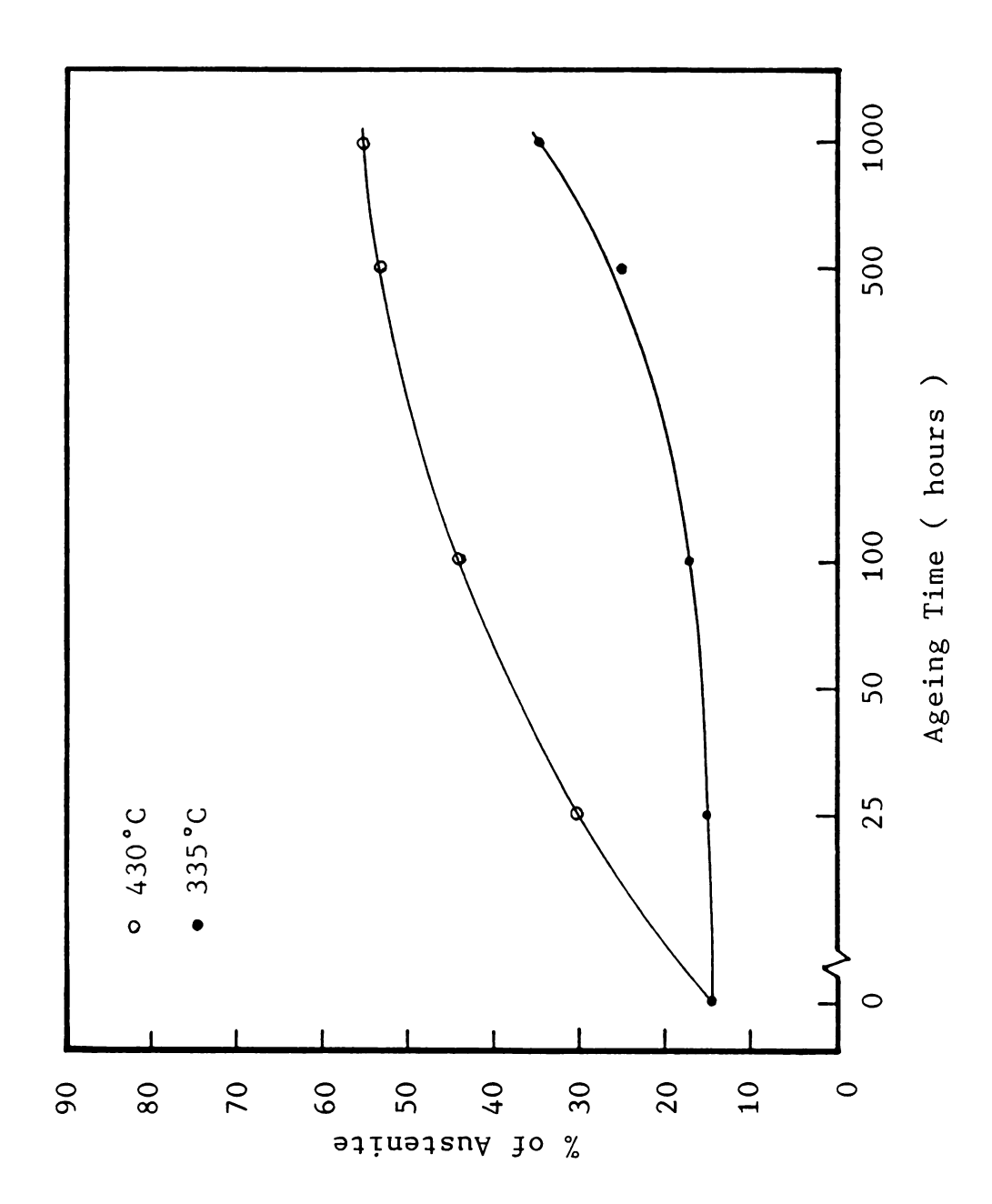


Figure 15. Volume fraction of austenite as a function of ageing time and ageing temperature.

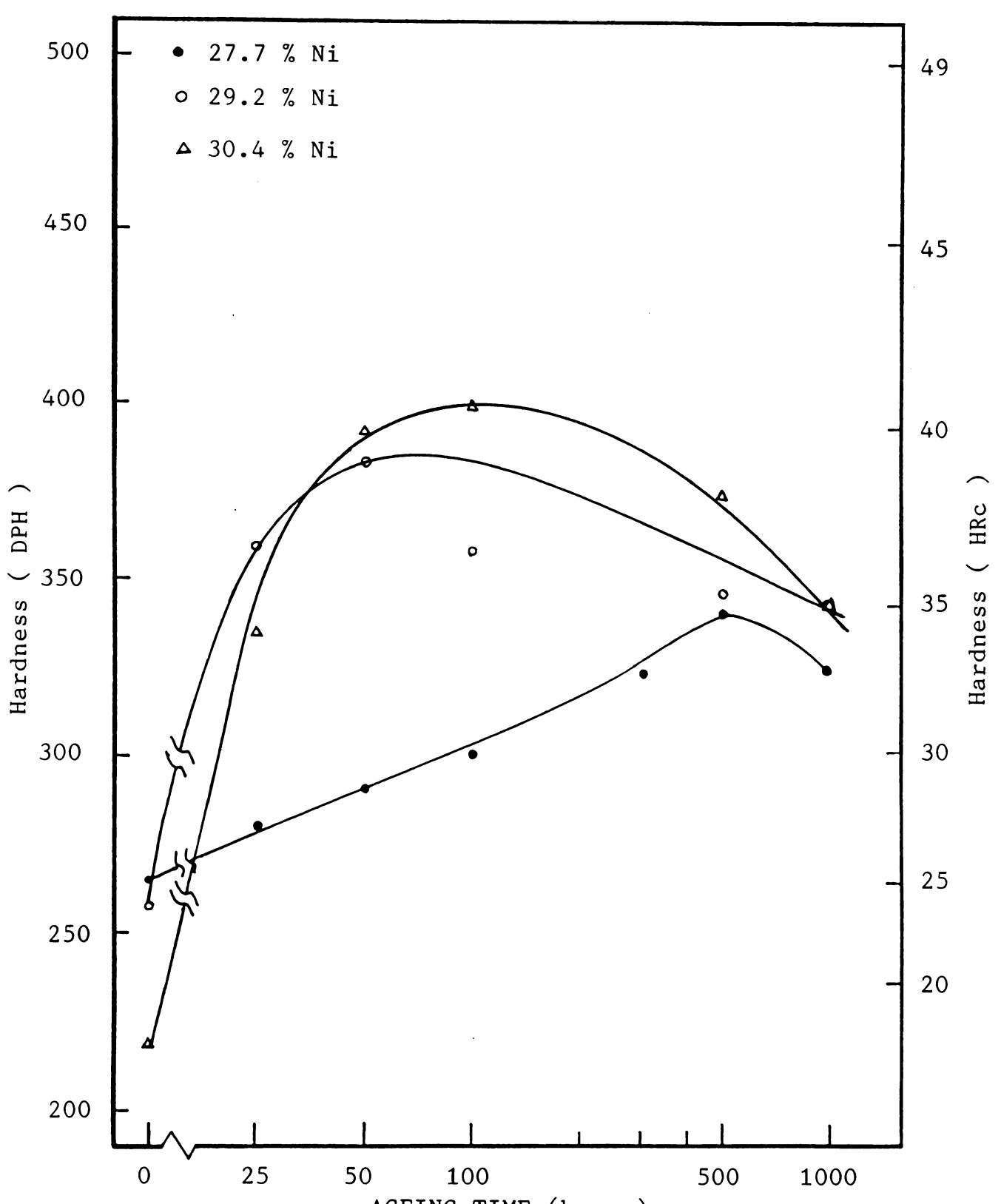


Table 2. Hardness response data of processing in Fe-30.4%Ni

I. Before	e ageing								
Condi	Hardı	Hardness		Condition				Hardness	
As-rece:	DPH :	DPH 151		Process A 70%C.R.			261		
After nor		104		Process B 10%C.R.				247	
As-quench	:	220		Process B 40%C.R.				257	
Process A		245		Process B 70%C.R.			270		
Process A	•	255		Process C 70%C.R.			280		
II. After	r ageing		1			1	71117		
Processes	% of	Ageing		Hardness (DPH) Ageing time (hours)					
	reduc- tion	temp.	25	)	50	100	50		1000
Α	10 %	335°C	335°C 28		-	305	36	5	413
		400°C	400°C -		354	358	391		-
		430°C	-		<b>.</b>	-	-		-
	/:() %	335°C	28	39	290	303	420		434
		400°C	36	56	396	413	409		388
		430°C	37	79	381	377	363		336
	70 %	335°C	335°C 29		314	331	36	0	394
		400°C	400°C 32		354	405 43		.9	404
		430°C	359		379	352	340		338
В	0%	200°C	22	28	230	234	24	2	270
		300°C	2.5	50	254	257	28	35	310
		335°C	25	56	260	267	30	)1	328
		400°C	°C 32		393	398	40	)6	410
		430°C	430°C 33		395	402	37	76	345

Table 2. (cont'd)

Processes	% of reduc- tion	Ageing temp. (°C)	Hardness (DPH)						
			Ageing Time (hours)						
			25	50	100	500	1000		
В .	10%	335	297	-	319	407	446		
		400	-	396	409	422	-		
	40%	335	292	295	313	415	456		
		400	386	417	425	417	415		
		430	425	424	406	394	365		
	70%	335	313	313	335	423	465		
		400	388	399	414	430	420		
		430	427	409	395	368	348		
С	70%	335	297	313	361	457	509		
		400	391	422	432	414	400		
		430	430	403	403	394	323		



AGEING TIME (hours)
Figure 16. Hardness responses of undeformed Fe-Ni alloys
as a function of ageing time and Ni content(430°C ageing).

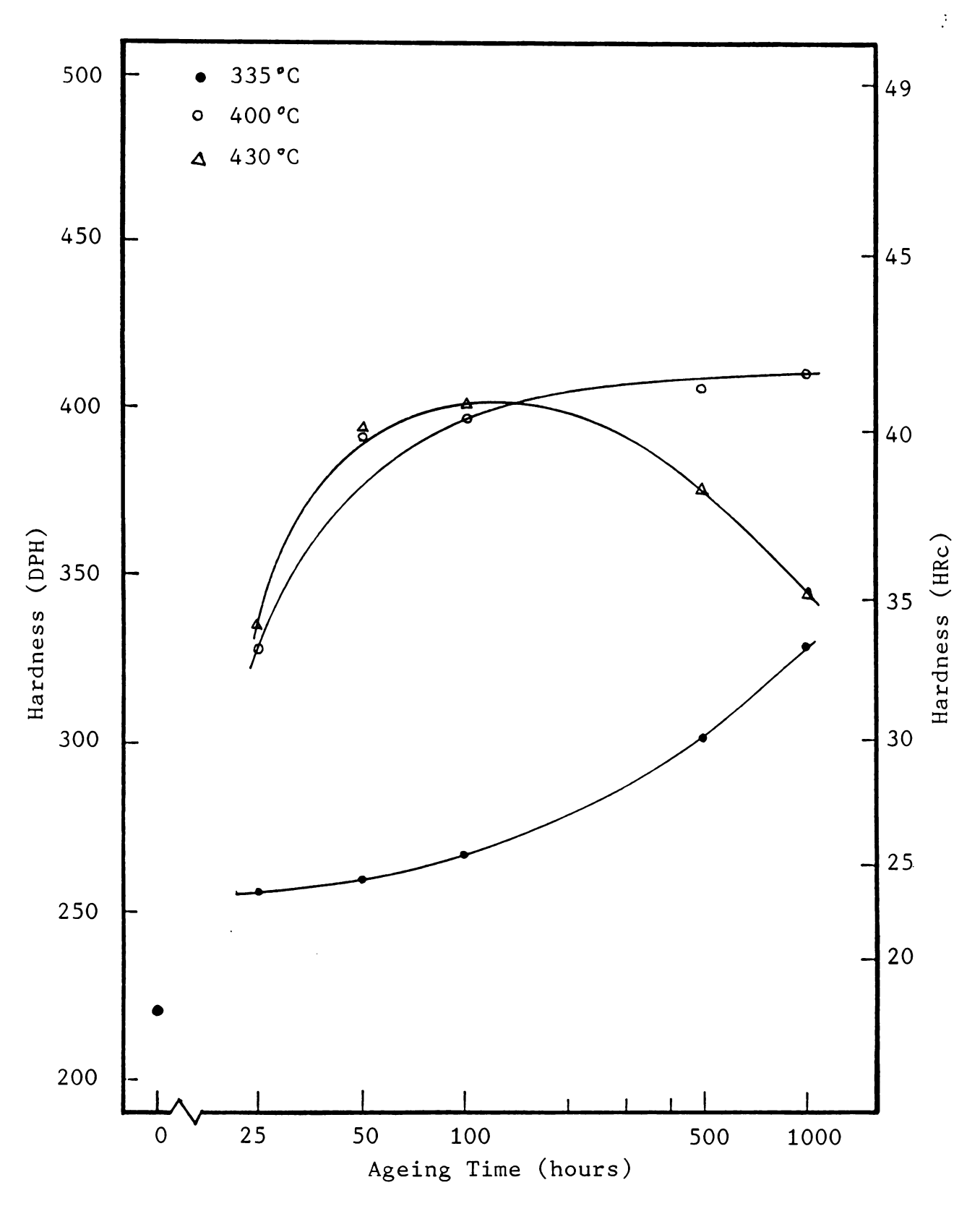


Figure 17. Hardness response of undeformed Fe-30.4%Ni as a function of ageing time and ageing temperature.

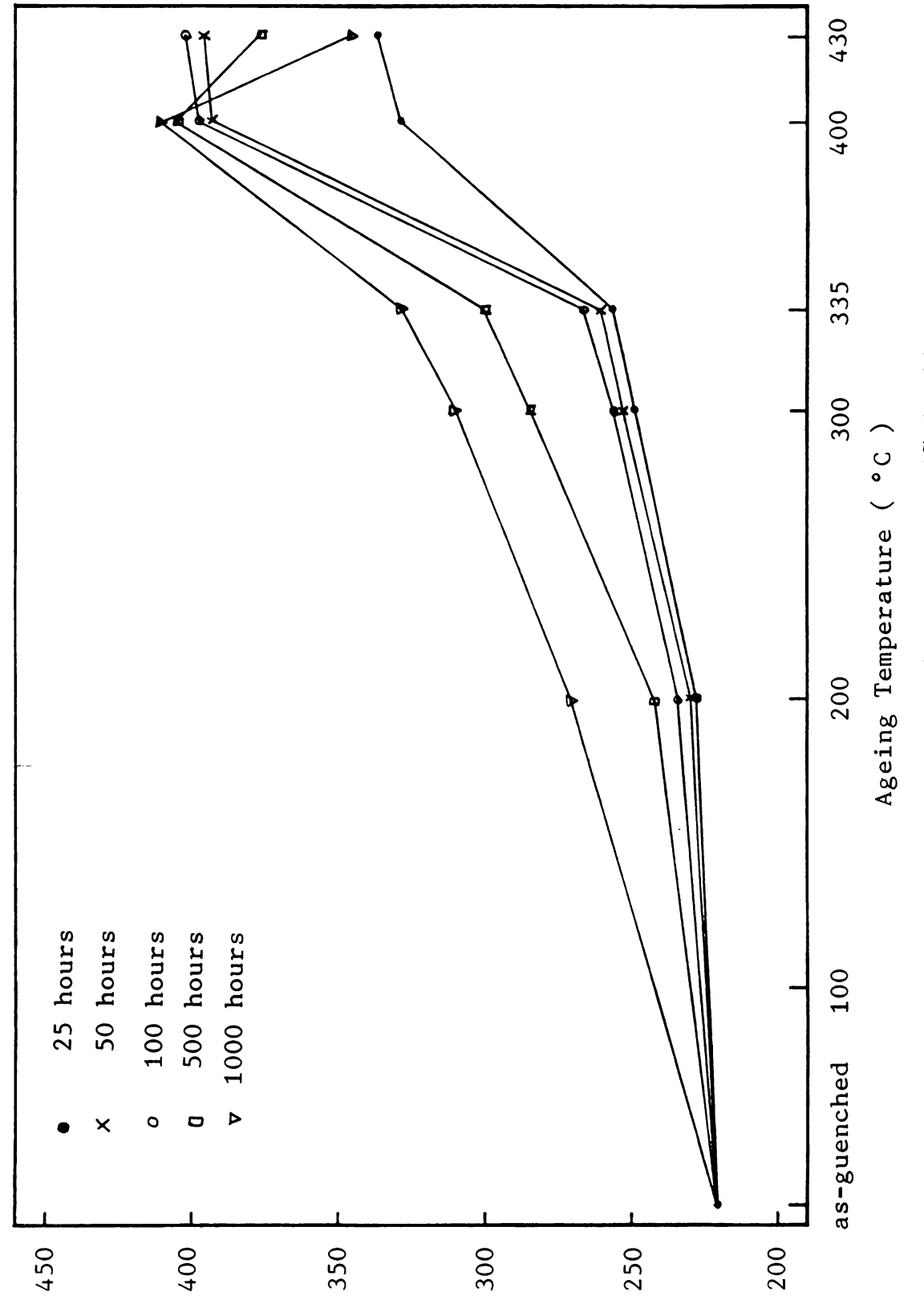


Figure 18. Hardness response of undeformed Fe-30.4%Ni alloy as a function of ageing temperature and ageing time.

time and ageing temperature. As expected, the time required to reach peak hardness decreases with increasing temperature. Moreover, the peak hardness obtained increases with decreasing ageing temperature. It can be seen that the hardness was increased more than 80% (from DPH 220 to 410) after ageing for 1000 hours at 400°C.

### 4-3-2 The Effect of Deformation

The hardness of Fe-Ni alloys did not change significantly on cold deformation, for example, after deformed 70 % in thickness the hardness was only increased 23 % for Fe-30.4%Ni alloy (Table 2).

Fig.19 & 20. show the effect of deformation on age-hardening in Fe-30.4%Ni alloy. The hardness of plastically deformed specimen after ageing is much larger than that of undeformed specimen, especially for specimen aged at 335°C. For example, the hardness of 70% deformed specimen was DPH 465 after ageing at 335°C for 1000 hours. While, the hardness of undeformed specimen was only DPH 328 after the same ageing treatment.

It is noteworthy that deformation as low as 10% has significant effect on the hardening. When compared to asquenched specimen aged at 335°C for 1000 hours, the increment in hardness for specimen with 10% deformation was DPH 118. On the other hand, the increment in hardness was only DPH 20 for 70%-deformed specimen as compared to the specimen with 10% deformation and aged at 335°C for 1000 hours.

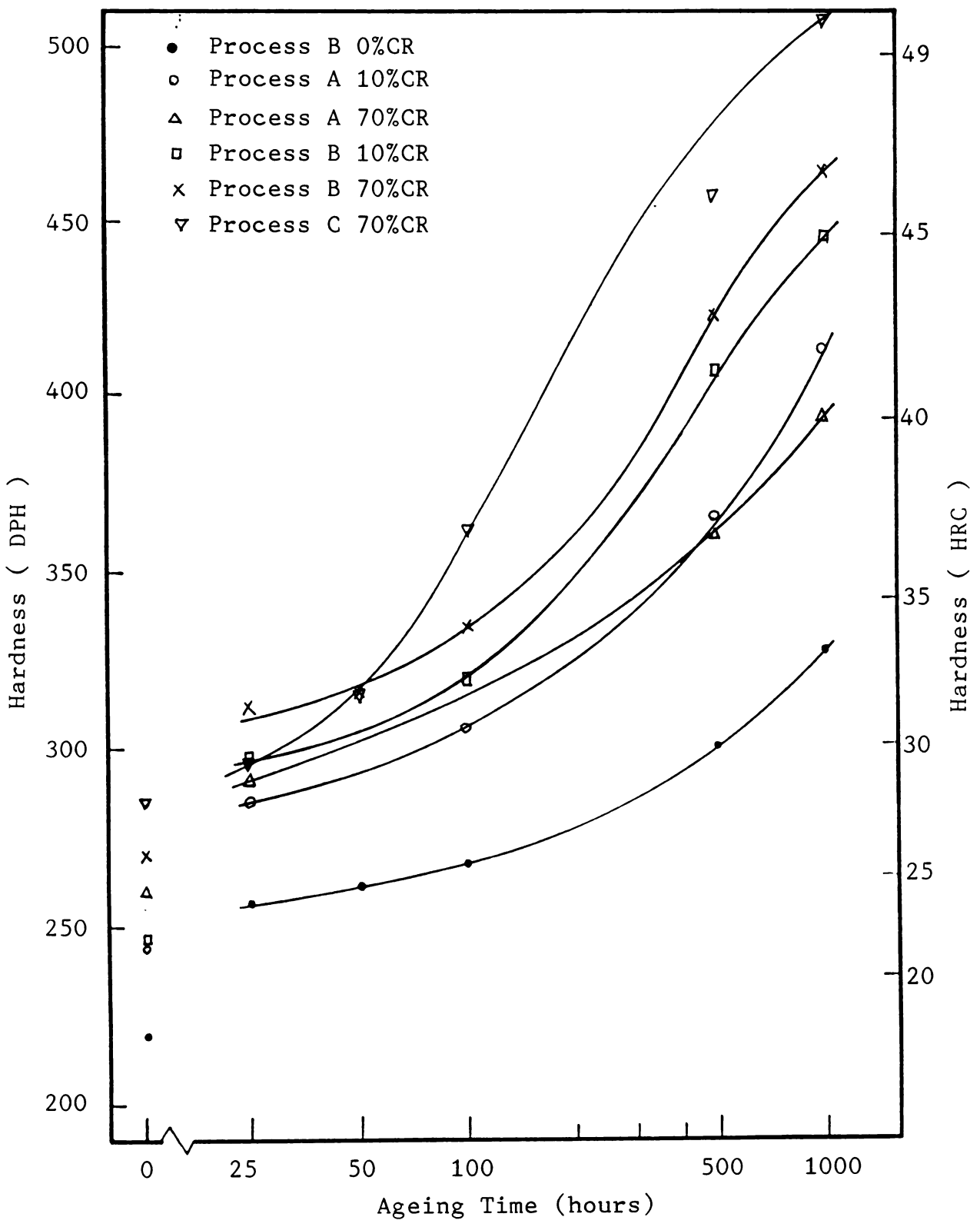


Figure 19. Hardness responses in Fe-30.4%Ni alloy under different processes and aged at  $335\,^{\circ}\text{C}$ .



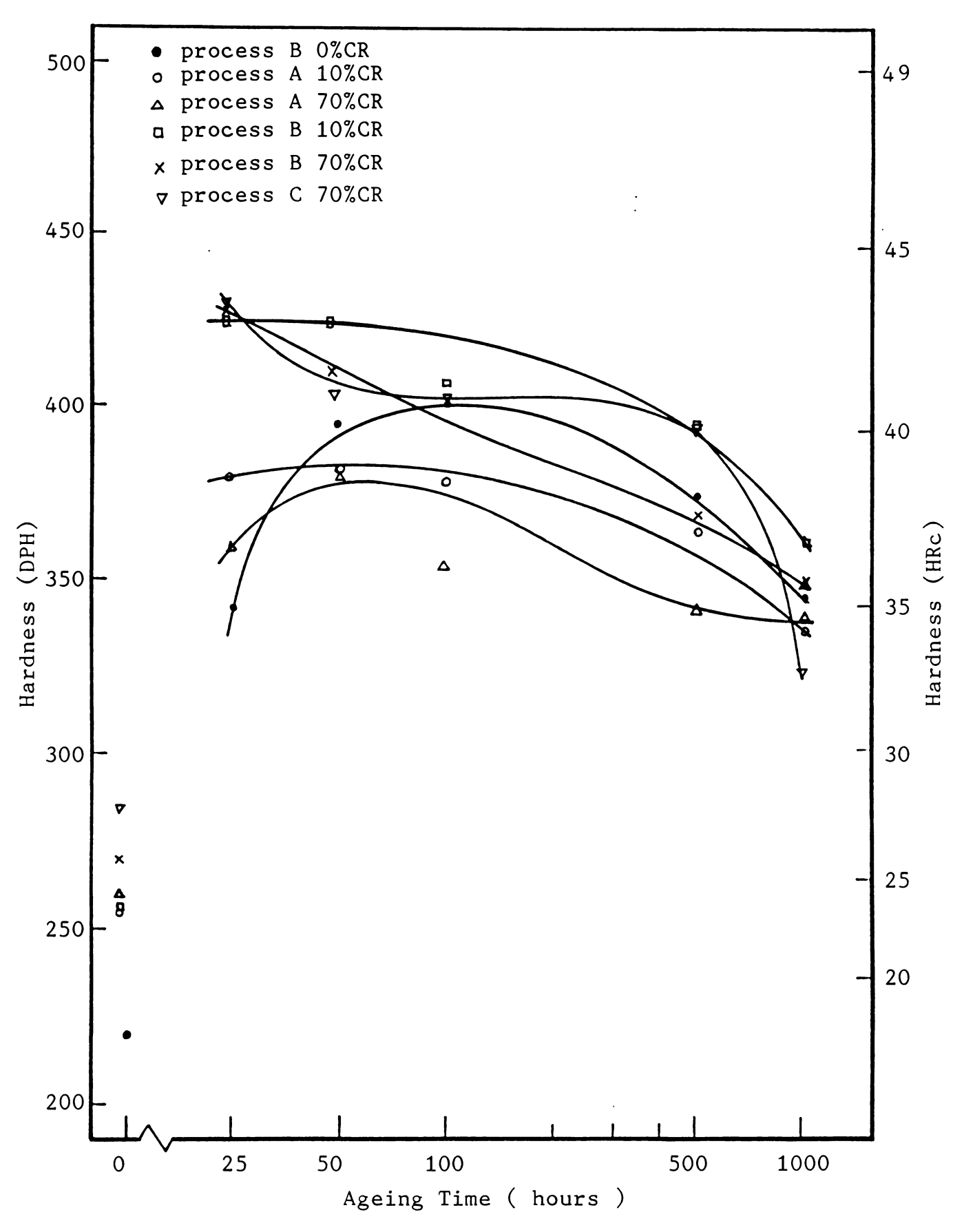


Figure 20. Hardness responses in Fe-30.4%Ni alloy under different processes and aged at 430°C.

As shown in Figure 20, the rate of hardening was also increased by deforming the specimen before ageing. Overageing occurred after ageing for less than 25 hours in deformed specimens when aged at 430°C. While for undeformed specimens, overageing did not occur until after ageing for 100 hours at the same temperature.

As shown in Fig.19, specimen which were quenched in liquid nitrogen and 70% deformed and requenched in liquid nitrogen can reach a highest hardness of DPH 509 after being aged at 335°C for 1000 hours. This hardness is also more than 80% higher than that of before ageing treatment. Fig. 19 & 20 also show that the age-hardening effect of process B is much better than that of process A. 4-4 Microstructures

## 4-4-1 Microstructures of Martensite

Figure 21 represents the optical microstructure of as-quenched specimens without any plastic deformation. It shows the typical plate martensites with midrib and twin substructure usually seen in Fe-Ni alloys with nickel content greater than 28 at% [23]. Figure 22. shows the TEM microstructure of the same specimen. The effect of deformation before and after quenching on the martensite morphology was shown in Figure 23 to 26. It is obvious that the martensite plates have been elongated along the rolling direction and became smaller and the dislocation density was increased. While, most of the midrib and twin substructure were disappeared. After requenching the





Figure 21. Optical microstructure of as-quenched Fe-30.4%Ni alloy

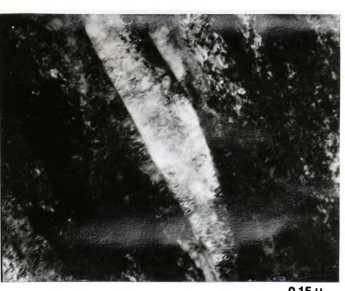


Figure 22. TEM microstructure of as-quenched Fe-30.4%Ni alloy



10 µ

Figure 23. Optical microstructure of martensite obtained by process A 70% cold rolled.



0.15 µ

Figure 24. TEM microstructure of martensite obtained by process A with 70% cold rolled.

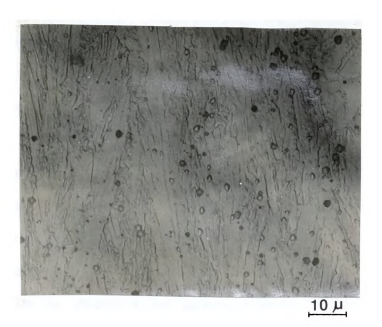
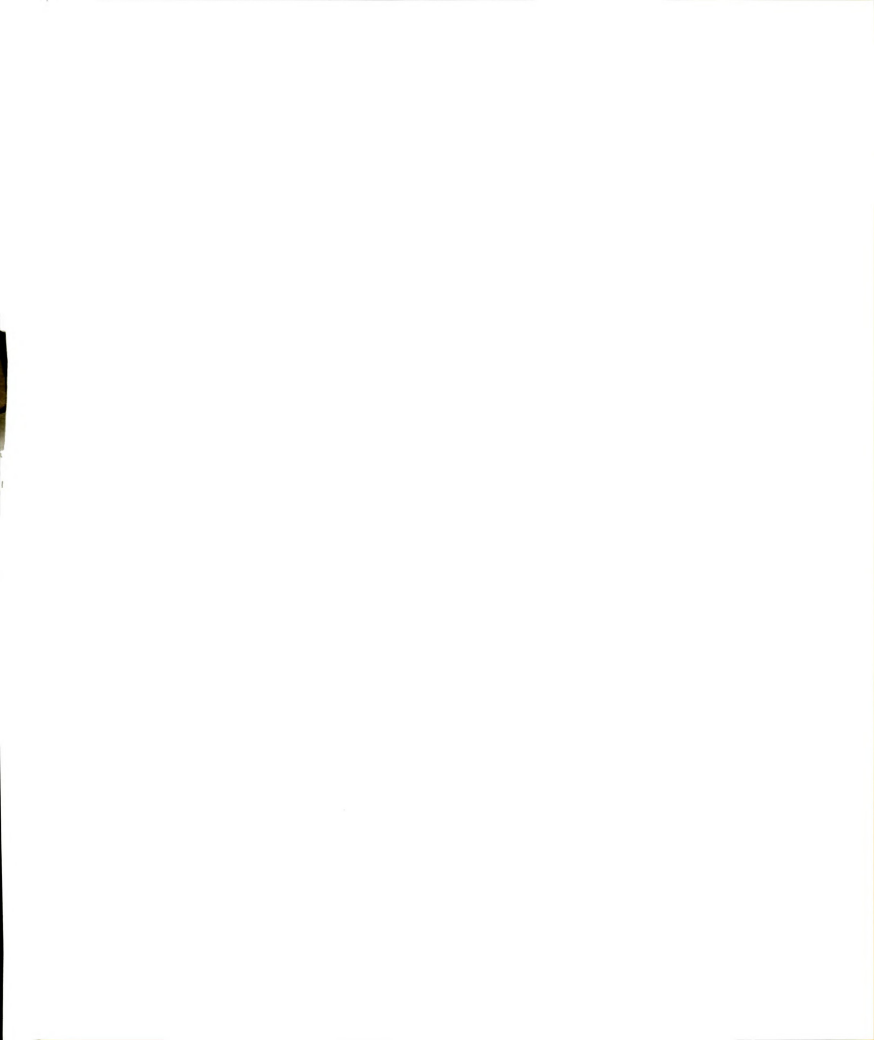


Figure 25. Optical microstructure of martensite obtained by process B with 70% cold rolling.



Figure 26. TEM microstructure of martensite obtained by process B with 70% cold rolling.



deformed martensite, twins were generated in some of the martensite plate (Figure 27). This may be the reason why the hardness of this microstructure is much higher.

4-4-2 The Effect of Ageing on Microstructures

For undeformed specimens, the microstructure did not show obvious change after being aged for 100 hours at 335°C. But after ageing for 500 hours at this temperature, many fine needle- or plate- like precipitates were formed throughout the martensite plate, as shown in Figure 28. The needle or plate like precipitates became denser and denser when increase the ageing time and many particle-shaped precipitates were also gradually formed in the martensite plates, as shown in Figure 29. Figure 30 shows the TEM microstructure of the undeformed sample after being aged for 1000 hours at 430°C. It can be seen that the plate-like and particle-shaped precipitates were coarser than those in Figure 29. Occasionally, cellular discontinuous precipitations were found in this specimen, as shown in Figure 31 and 32.

For 70% deformed sample of process A, same kind of precipitates as those in the undeformed sample were formed in the martensite plates after ageing for 1000 hours at 335°C.

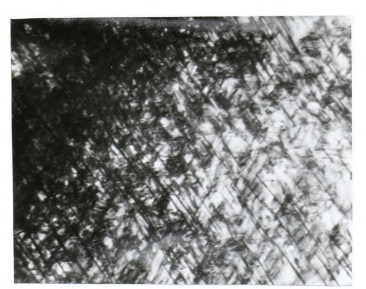
Only the precipitates and the martensite plates are much finer in the deformed specimens, as shown in Figure 33.

The main differences in microstructure between specimens deformed after and before quenching then ageing at 335°C for 1000 hours are that the martensite plates are much thinner and finner for specimen deformed after



0.15 µ

Figure 27. TEM microstructure of martensite obtained by process C with 70% cold rolling.



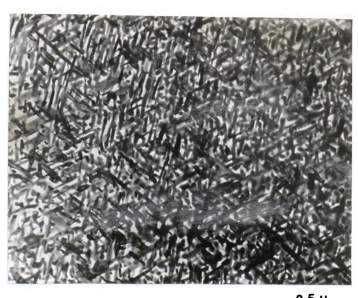
0.17µ

Figure 28. Precipitates formed in the martensite after ageing the undeformed sample at 335°C, 500h.



0.25

Figure 29. Typical precipitates formed after ageing at 335°C for 1000 hours.



0.5 µ

Figure 30. Precipitates were coarsened when aged at  $430\,^{\circ}\mathrm{C}$  for 1000 hours.



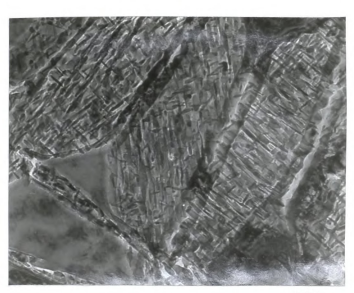
2.5 µ

Figure 31. Cellular precipitation in an Fe-30.4%Ni aged at  $430\,^{\circ}\text{C}$  for 1000 hours.(TEM)



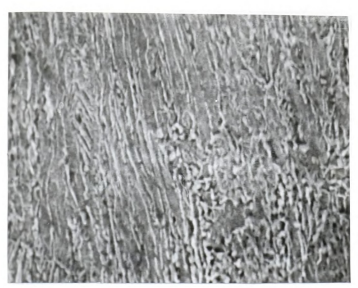
1.3 µ

Figure 32. Cellular precipitation in an Fe-30.4%Ni aged at  $430\,^{\circ}\text{C}$  for 1000 hours.



0,2 µ

Figure 33. Microstructure of aged Fe-30.4%Ni martensite process A with 70% cold rolling, aged at 335°C, 1000 h.



1.3 µ

Figure 34. SEM microstructure of aged martensite, process B with 70% cold rolling, aged at  $335^{\circ}\text{C}$ , 1000~h.

quenching and the precipitates formed in the martensite plate boundaries are much more for this specimen, as shown in Figure 34.

Figure 35 shows the microstructure of a specimen requenched after 70 % deformation and aged at 335°C for 1000 hours. It also shows a lot of precipitates formed in the martensite plate boundaries. The precipitates inside the martensite plates were very fine and cannot be resolved in SEM as in the case of Figure 34.

#### 4-4-3 Formation of Austenite

As shown in Figure 15, the amount of austenite reformed at the ageing temperature continuously increases as the ageing time is increased. When aged at a temperature below the As temperature, as in the case of ageing a 70 % deformed sample of process B at 430°C, the austenite appears to be formed by diffusional process and not that generated by a reverse shear transformation, as shown in Figure 36 and 37. On the other hand, when aged at a temperature above the As temperature, as in the case of ageing a 70 % deformed sample of process A at 430°C, two kinds of austenites were formed, one kind is formed by diffusional process and the other kind is formed by diffusionless process, as shown in Figure 38 and 39.

#### 4-4-4 Identification of Precipitates

During ageing, precipitates were formed in the grain boundaries (Figure 31,32,40), in the martensite cell wall (Figure 34), and in the martensite plates (Figure 27,28,29). Analyze the SAD pattern of the cellular precipitates shown in

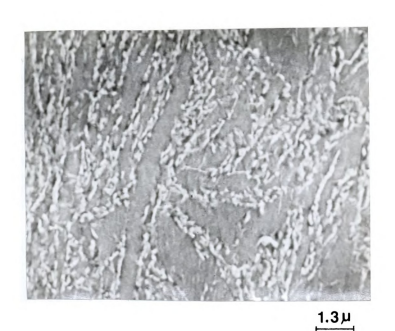


Figure 35. SEM microstructure of aged martensite, process C with 70% cold rolling, aged at  $335\,^{\circ}$ C, 1000 h.

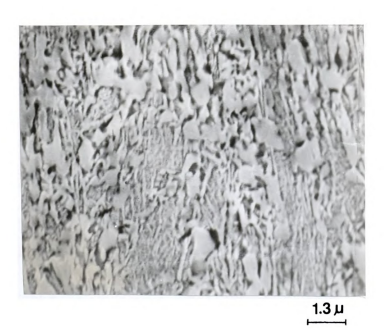


Figure 36.Austenite formed by diffusional process process B, aged at 430°C for 1000 hours.

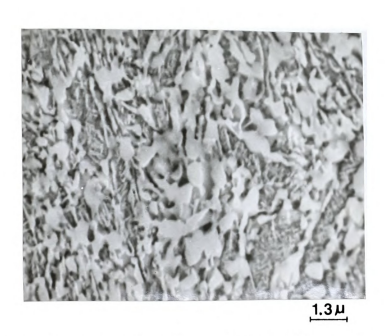


Figure 37. Austenite formed by diffusinal process, after ageing at  $430\,^{\circ}\text{C}$  for 1000 hours in process C.



1.3 μ

Figure 38. Austenite formed by diffusionless and diffusional processes, after ageing at  $430\,^{\circ}\text{C}$  for 1000 hours in process A.

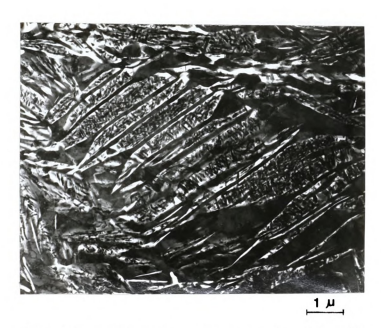


Figure 39. TEM microstructure of Fe-30.4%Ni alloy shows austenite formed by diffusionless process after aged at 430°C for 1000 hours in process A.

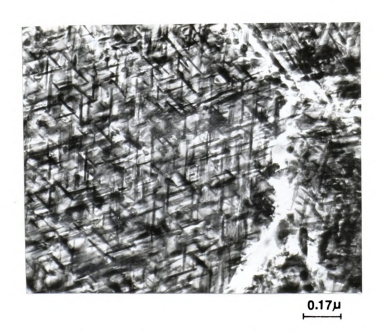


Figure 40. Precipitates formed in the grain boundary.

Figure 31, these precipitates turned out to be austenites. The precipitates formed in the martensite plates after ageing are very similar in shape for different processing. Examining these precipitate plates carefully, it can be found that these plates grow in three preferential directions, as shown in Figure 28 and 29. The selected area diffraction (SAD) pattern of these precipitates were quite complex. Determination of crystal structure of these precipitates require further investigation.

### CHAPTER FIVE

### DISCUSSIONS

### 5-1 The Effect of Deformation on The As Temperature

By using a thermodynamic approach, we can explain reverse martensitic transformation. From the thermodynamics' point of view, the reverse martensitic transformation will not occur until the martensite is heated to a temperature As, which the free energies of the austenite is lower than that of the martensite, as shown in Figure 41. This is because that for Fe-Ni alloys of high Ni content there exists a large temperature hysteresis in the martensite-austenite transformation cycle. And the existance of the temperature hysteresis means there is a energy barrier (activation energy) which must be overcome before the transformation can occur. The As temperature will then either decrease or increase with deformation depends on whether the free energy of the martensite increase or decrease with deformation. If the free energy of martensite increase (decrease) with deformation, As naturally decrease(increase) with will temperature deformation, as illustrated in Figure 41.

In general, the origin of the dependence of As

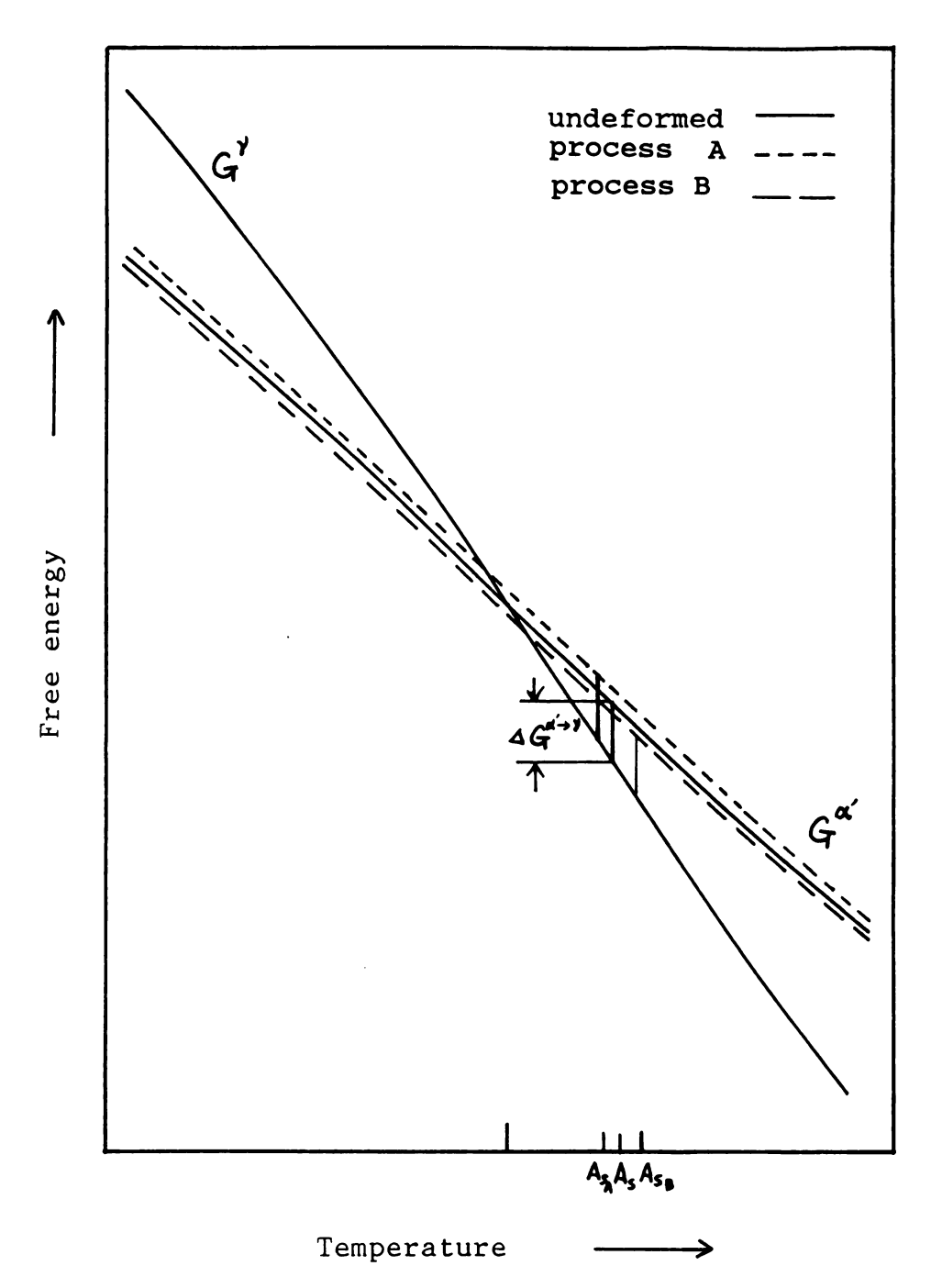


Figure 41. The free energy of Fe-Ni martensite and austenite as a function of temperature (Schematic)

temperature on the deformation can be interpreted on the basis of either the ease of nucleation or interface propagation.

It has been indicated [8] that dislocation motion required for reverse martensitic transformation. effect of deformation on the As temperature can be interpreted by the interface propagation model and two nucleation models. nucleation of new austenite depends on dislocation motion, an increase in deformation would hinder dislocation motion through tangling, thus reduc- ing the ease of austenite nucleation, and therefore As would be raised. On the other hand, nucleation can also be interpreted as requiring a specific dislocation array. Deformation would increase the density of dislocation and form strain centers where these dislocation can lower their free energies by forming austenite this model predicts a decrease nuclei. Hence, in temperature. The observed results in the present study can be explained by either of these two models. The first model can explain the case of deforming the Fe-Ni martensitic alloy ( quenched + deformed ). While the second model can explain the case of deforming the Fe-Ni austenitic alloy ( deformed + quenched ). As stated previously, many researchers observed that reversed austenite initiates along the martensite plate periphery and the martensite-austenite interface. Thus the reverse martensitic transformation may depend propagation of the original martensite-austenite interface. When deformation is applied to the alloy the dislocation density increases. Hence, a higher energy barrier is formed, which means a larger driving force is needed for interface propagation. As a result, the As temperature is increased.

# 5-2 The Effect of Ageing on The As and Af Temperatures

As shown in Figure 7, the As temperature increases with the ageing time. This is the direct result of either the formation of austenite or precipitates during ageing. The Ni content in martensite will decrease as the amount of equilibrium austenite phase increases or if the precipitates are Ni-rich compounds. Therefore, from Figure 3 it is clear that As temperature would increase with the ageing time. On the other hand, the Af temperature is almost constant after ageing for 100 hours at 335°C. This is beacuse the amount of transformed austenite is relatively small, and have little effect on the Af temperature. On further ageing, Af increases with the ageing time as a result of a larger amount of austenite formed.

When aged at 430°C, which is above the As temperature for undeformed sample, it is expected that certain amount of austenite will be formed diffusionlessly in a short time and then more austenite will be formed diffusionally after sufficient time. This is exactly what the result of X-ray and microstructure shows ( Figure 15 and 31 ). Thus the Ni content in the martensite will decrease even for a relatively short ageing time. As a result, the As temperature of the sample will increase promptly, as observed in this study.

# 5-3 The Effect of Deformation on the Enthalpy Change

The enthalpy change of reverse martensitic transformation decreased with deformation in both process A and process B, as shown in Figure 14. Only the decrease in enthalpy change was less for process A. This effect can be tentatively interpreted by the decrease in the volume fraction of martensite due to deformation. In the case of process A, deformation was performed in the austenite state at room temperature ( within the two phase temperature region ), the austenite was possible to decompose to equilibrium austenite by deformation. When subsequently cool this sample in liquid nitrogen, the volume fraction of martensite will be less than that of undeformed sample. Therefore, the enthalpy change of reverse martensitic transformation will decrease with deformation. In the case of process B, deformation was performed in the martensite state at room temperature, some of the martensite were decomposed to equilibrium austenite after deformation. Thus, the volume fraction of martensite decreased with deformation. result, the enthalpy change of reverse transformation decreased with deformation.

# 5-4 Age-hardening Mechanism

During ageing the hardening effect is the combination of three seperate processes: (1) the formation of precipitates, (2) recovery of defect structure of martensite and grain refinement, (3) the formation of austenite.

In this study, there is no obvious evidence of recovery

and grain refinement. Thus, the observed results are due to the formation of precipitates. Because the precipitate plates or particles nucleate on dislocations and by pinning the dislocation, prevent the dislocations from rearranging themselves into low-angle boundaries. Therefore, the strengthening of this alloy due to grain refinement is almost neglecgible.

The formation of austenite seems to be an important part of the ageing process in this alloy. As stated previously, the austenite can be formed by two different processes depending the ageing temperature. However, the formation of on austenite will generally decrease the hardness of the alloy. Therefore, the age-hardening of Fe-30.4%Ni alloy seems to be accomplished by the formation of very fine and precipitates. The precipitates nucleate on dislocations and then grow. The size and amount of precipitates depend on the dislocation density. Because the dislocation density is increased after deformation, the nuclei density of the precipitates formed during ageing are higher in the deformed sample. As a result, the precipitates are finer and denser. This corresponds to the higher hardness response of ageing in Although it is possible that the the deformed sample. "precipitates" are austenite formed through a discontinuous electron diffraction patterns indicate a more reaction, complex crystal structure of these precipitates. Determination of crystal structure of these precipitates will require further investigation.

## CHAPTER SIX

### CONCLUSIONS

Three kinds of thermomechanical treatments were performed in this study. After thermomechanical treatment, the Fe-30.4%Ni alloy had the following calorimetric and hardness responses:

- (1) The As and Af temperatures of reverse transformation were shifted to higher temperature side after ageing, as a result of the formation of austenite and precipitates.
- (2) Deformation will either increase or decrease As temperature, depending on the process performed. If deformation was performed before quenching, the As temperature will decrease. On the other hand, if deformation was done after quenching, the As temperature will increase. The effect of deformation on the As temperature can be interpreted by using the thermodynamics approach and by the interface propagation model and nucleation models.
- ( 3 ) The enthalpy change of reverse transformation ( martensite to austenite ) was decreased after deforming the alloy.
- (4) The Fe-30.4%Ni alloy used in this study can be hardened remarkably after deformation and ageing. Process C had the

highest hardness response when aged at 335°C for 1000 hours. The hardness can be increased as much as 80 %.

- (5) No evidence of grain refinement due to ageing at a temperature either below or above the As temperature were found in the present study.
- (6) The age-hardening of the Fe-30.4% Ni alloy was accomplished by the formation of fine and dense plate-like and particle-shaped precipitates. It was not possible to identify the crystal structure of these precipitates.



#### BIBLIOGRAPHY

- E.A. Owen and A.H. Sully, "The Equilibrium Diagram of Iron-Nickel Alloys", <u>Philophical Magazine</u>, series 7, 1939, vol. 27, p.614.
- 2. E.A. Owen and Y.H. Liu, "Further X-Ray Sturdy of the Equilibrium Diagram of the Iron-Nickel System", J. Iron Steel Inst., Oct. 1949, Vol. 163, p.132.
- 3. J.I. Goldstein and R.E. Ogilvie, "A Re-evaluation of the Iron-Rich Portion of the Fe-Ni System", TMS-AIME, 1965, vol. 233, p.2083.
- 4. A.D. Romig and J.I. Goldstein, "Determination of the Fe-Ni and Fe-Ni-P Phase Diagrams at Low Temperatures (700 to 300 C)", Met. Trans., 1980, Vol.11A, p.1151.
- 5. V.T. Heumann and G. Karsten, "Karbonylverfahren and Aufdampfverfahren zur Bestimmung von Phasengleichgewichten im Temperaturbereich geringer Beweglichkeit am Beispiel der Eisen-Nickel-Legierungen", Archiv fur das Eisenhuttenwesen, 1963, vol 34, p.781.
- Kaufman and M. Cohen, "The Martensitic Transformation in the Iron-Nickel System", <u>TMS-AIME</u>, 1956, vol 206, p.1393.
- 7. M.J. Roberts and W.S. Owen, "The Strength of Martensitic Iron-Nickel Alloys", <u>Trans. ASM</u>, 1967, vol 60, p.687.
- 8. L.E. Pope, "The Effect of Plastic Deformation on the Martensite-to-Austenite Transition in an Iron-Nickel Alloy", Met. Trans., 1972, vol. 3, p.2151.
- 9. M.Enomoto and E. Furubayashi, "Microduplex Structures Originating from deformed Fe-Ni Martensite", <u>Materials Sci. and Engin.</u>, 1976, vol. 24, p.123.
- 10. R.L. Miller, "Ultrafine-Grained Microstructures and Mechanical Properties of Alloy Steels", <u>Met. Trans</u>, 1972, vol. 3, p.905.
- 11. H. Chang, S. Sastri and B. Alexander, "A Comparison of Enthalpy Change Between  $\alpha' \rightarrow \gamma$  and  $\alpha \rightarrow \gamma$  Transformations in Fe-Ni Alloys", Acta Metallurgica, 1980, Vol. 28, p.925.

- 12. R.L. Miller and W.C. Leslie, "AGE HARDENING IN BINARY MARTENSITIC Fe-Ni Alloys", Scripta Metallurgica, 1978, vol. 12, p.1125.
- 13. L. Kaufman and H. Nesor, "Calculation of the Binary Phase Diagrams of Iron, Chromium, Nickel and Cobalt", <u>Z. fur Metal.</u>, 1973, vol. 64, p.249.
- 14. J.E. Albertsen, G.B. Jensen and J.M. Knudsen, "Structure of taenite in two iron meteorites", <u>Nature</u>, 1978, vol. 273, p.453.
- 15. F.W. Jones and W.I. Pumphrey, "Free Energy and Metastable States in the Iron-Nickel and Iron-Manganese Systems", J. Iron and Steel Inst., 1949, vol. 163, p.121.
- 16. Z. Nishiyama, "Conditions for Martensite Formation and Stabilization of Austenite" in "Martensitic Transformation", ed. by M. Fine et al., Academic Press, 1978, p.263.
- 17. L. Kaufman and M. Cohen, "Thermodynamics and Kinetics of Martensitic Transformations", <u>Progress in Metal Physics</u>, 1958, vol. 7, ed. by B. Chalmers and R. King, Pergamon Press.
- 18. S.Jana and C.M. Wayman, "Martensite-to-FCC Reverse Transformation in an Fe-Ni Alloy", TMS-AIME, 1967, vol. 239, p.1187.
- 19. G.Krauss and M. Cohen, "Strengthening and Annealing of Austenite Formed by the Reverse Martensitic Transformation", TMS-AIME, 1962, vol. 224, p.1212.
- 20. B. Hyatt and G. Krauss, "Cyclic Transformation in Fe-Ni-C Alloys", Trans. of ASM, 1968, vol. 61, p.168.
- 21. H. Kessler and W. Pitsch, "On the nature of martensite to austenite reverse transformation", <a href="Acta Metallurgica">Acta Metallurgica</a>, 1967, vol. 15, p.401.
- 22. S.V. Radeliffe and E.B. Kula, "Deformation, Transformation and Strength", <u>Fundamentals of Deformation Processing</u>, Syracuse Univ. Press, Syracuse, 1964, pp.321-363.
- 23. R.L. Miller, "A Rapid X-Ray Method for the Determination of Retained Austenite", <u>Trans. of ASM</u>, 1964, Vol. 57, pp.892-899.



